SEMMELWEIS EGYETEM

DOKTORI ISKOLA

Ph.D. értekezések

3312.

VARGA NOÉMI NÓRA

Bőrgyógyászat és venerológia

című program

Programvezető: Dr. Sárdy Miklós, egyetemi tanár

Témavezetők: Dr. Kiss Norbert, egyetemi adjunktus és

Dr. Medvecz Márta, egyetemi docens

INNOVATIVE MULTIMODAL IMAGING TECHNIQUES IN DERMATOLOGY

Ph.D. Thesis

Noémi Nóra Varga M.D.

Translational Medicine Program

Károly Rácz Conservative Medicine Doctoral School

SEMMELWEIS UNIVERSITY

Supervisors: Norbert Kiss, M.D., Ph.D.

Márta Medvecz, M.D., Ph.D.

Official reviewers: Prof. Lajos Kemény, M.D., Ph.D., D.Sc.

Roxana-Ioana Nedelcu, M.D., Ph.D.

Head of the Complex Examination Committee: Andrea Harnos, M.D., Ph.D.

Members of the Complex Examination Committee:

Prof. Alan Irvine, M.D., Ph.D., D.Sc.

Prof. Szekanecz Zoltán, M.D., Ph.D., D.Sc.

Budapest

2025

"The skin is not only a barrier but a window - revealing internal processes when examined with the right tools."

- *Dr. Thomas B. Fitzpatrick*

TABLE OF CONTENT

1 LIST OF ABBREVIATIONS

A.U. Arbitrary Unit

AAD American Academy of Dermatology

AF Autofluorescence (MSI channel)

AI Artificial Intelligence

ALM Acral Lentiginous Melanoma

AUC Area Under the Curve (in the context of ROC curve)

CENTRAL Cochrane Central Register of Controlled Trials (a bibliographic database of controlled trials maintained by the Cochrane Collaboration)

CI Confidence Interval

DF Dermatofluoroscopy

DOI Digital Object Identifier

DOR Diagnostic Odds Ratio

DSC Dermoscopy

DSC+AI Dermoscopy combined with Artificial Intelligence

EADO European Association of Dermato-Oncology

EMBASE Excerpta Medica Database (a biomedical and pharmacological bibliographic database produced by Elsevier)

G Green (MSI channel)

GRADE Grading of Recommendations Assessment, Development and Evaluation (a tool for grading the quality of evidence)

HFUS High-Frequency Ultrasound

IR Infrared (MSI channel)

LMM Lentigo Maligna Melanoma

LMM sec. nod. Lentigo Maligna Melanoma with secondary nodular component

MEDLINE Medical Literature Analysis and Retrieval System Online (the bibliographic database of the National Library of Medicine)

MHz Megahertz

MPM Multiphoton Microscopy

MSD Multimodal Spectral Diagnosis

MSE Mean Squared Error

MSI Multispectral Imaging

MSI+AI	Multispectral Imaging combined with Artificial Intelligence
NCCN	National Comprehensive Cancer Network
NIH	National Institute of Health
NIR-SI	Near-Infrared and Skin Impedance (spectroscopy)
NM	Nodular Melanoma
NPV	Negative Predictive Value
OCT	Optical Coherence Tomography
OG-HFUS	Optically Guided-High-Frequency Ultrasound
PIRD	Population–Index test–Reference test–Diagnosis (a framework for formulating scientific questions)
PPV	Positive Predictive Value
PRISMA	Preferred Reporting Items for Systematic Reviews and Meta-Analyses
PROSPERO	International Prospective Register of Systematic Reviews
QUADAS-2	Quality Assessment of Diagnostic Accuracy Studies included in the Systematic Reviews, version 2. (a tool to assess the study quality and risk of bias)
R	Red (MSI channel)
RCM	Reflectance Confocal Microscopy
ROC	Receiver Operating Characteristics (curve)
ROI	Region Of Interest
RS	Raman Spectroscopy
SD	Standard Deviation
SLNB	Sentinel Lymph Node Biopsy
sROC	summary Receiver Operating Characteristics (curve)
SSM	Superficial Spreading Melanoma
SSM sec. nod.	Superficial Spreading Melanoma with secondary nodular component
TeleDSC	Teledermoscopy
UC	Unclassified (melanoma subtype)
UV	Ultraviolet

2 STUDENT PROFILE

2.1 Vision and mission statement, specific goals

My vision is a world where skin cancer poses no significant threat to life, and patients benefit from accurate diagnoses and effective treatments that enhance survival rates. Therefore, my mission is to promote the implementation of novel non-invasive imaging technologies in everyday dermatological practice. My specific goal is to elevate melanoma diagnostics to the highest standard possible, enhancing early detection, ensuring faster treatment, and improving prognosis for patients worldwide.

2.2 Scientometrics

Number of all publications:	7
Cumulative IF:	17.5
Av IF/publication:	3.5
Ranking (SCImago):	D1: -, Q1: 5, Q2: -
Number of publications related to the subject of the thesis:	2
Cumulative IF:	7.6
Av IF/publication:	3.8
Ranking (Sci Mago):	D1: -, Q1: 2, Q2: -
Number of citations on Google Scholar:	28
Number of citations on MTMT (independent):	9
H-index:	4

The detailed bibliography of the student can be found on pages 80-82.

2.3 Future plans

Building on the findings of my thesis, future work will focus on further developing and validating non-invasive imaging technologies to improve early melanoma detection and staging accuracy. I plan to expand my research in melanoma diagnostics by utilizing my acquired knowledge and skills in this area. A promising future direction for my research would be to explore the efficacy of multimodal imaging in clinical settings as well.

I believe that healthcare requires a blend of hands-on clinical experience and academic insight; therefore, I strive to incorporate what I have learned in my academic work into my residency training. With the cohesion of my research and clinical experiences, my specific goal is to build a professional path that raises melanoma care to the highest possible level, thereby improving the prognosis for patients.

3 SUMMARY OF THE THESIS

Melanoma is one of the most aggressive forms of skin cancer, and accurate early diagnosis is essential for improving patient outcomes. The histopathological Breslow thickness remains the most important prognostic factor for melanoma; however, it is unavailable at the time of initial clinical diagnosis. In this thesis, our aim was to compare the performance of non-invasive optical imaging techniques to improve melanoma diagnosis, with a particular focus on estimating Breslow thickness preoperatively with two entirely novel prototype devices that are not yet in routine clinical use.

In the first part of our research, we conducted a single-center prospective validation study comparing two novel imaging modalities: optically guided high-frequency ultrasound (OG-HFUS) and multispectral imaging (MSI). A total of 101 patients with histologically confirmed primary melanomas were enrolled. OG-HFUS demonstrated significantly higher diagnostic performance compared to MSI in estimating Breslow thickness, with almost perfect agreement with histological findings. This supports the implementation of OG-HFUS as a reliable, non-invasive tool for preoperative melanoma staging.

In the second part of the thesis, we performed a systematic review and meta-analysis of 141 studies, synthesizing diagnostic accuracy data for various non-invasive optical imaging modalities. Our meta-analysis found that reflectance confocal microscopy (RCM) and dermoscopy combined with artificial intelligence (DSC+AI) reached the highest sensitivity, while multispectral imaging combined with artificial intelligence (MSI+AI) also demonstrated promising diagnostic performance. Based on our results, both RCM and DSC+AI can serve as second-step optical evaluation methods for suspicious lesions following initial screening with dermoscopy (DSC). The integration of artificial intelligence into imaging workflows consistently improved diagnostic accuracy.

Together, these studies emphasize the growing role of non-invasive, multimodal, and AI-supported imaging in melanoma care. We recommend incorporating OG-HFUS into standard preoperative workflows and supporting the wider adoption of validated AI-assisted imaging systems. By maintaining a strong emphasis on multimodal imaging, healthcare providers could improve early detection and outcomes for patients with melanoma.

4 GRAPHICAL ABSTRACT

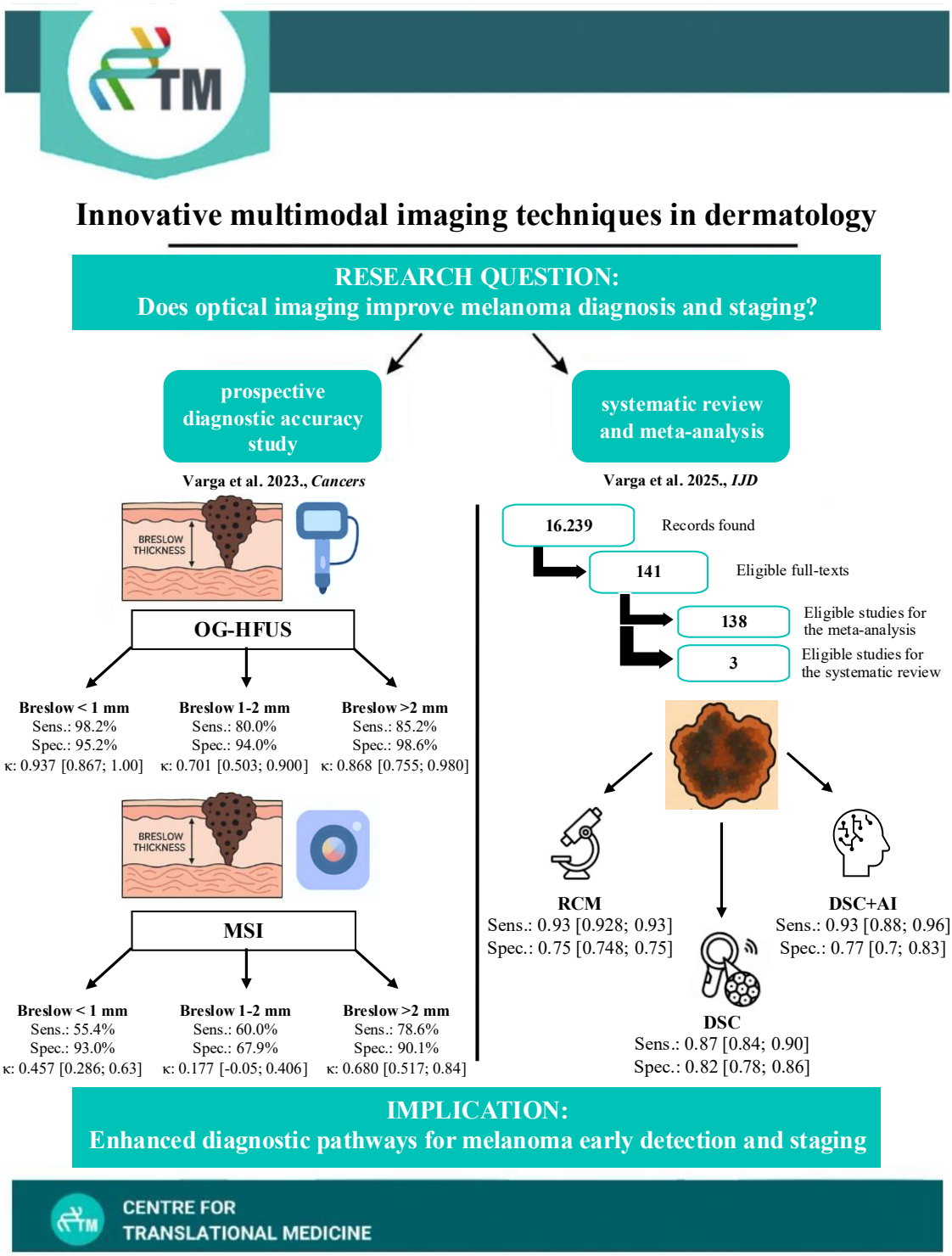

5 INTRODUCTION

5.1 Overview of the topic

5.1.1 What is the topic?

The focus of my research is to investigate the diagnostic performance of emerging non-invasive optical imaging techniques for melanoma diagnosis, with a particular focus on preoperative Breslow thickness assessment, to identify clinically useful tools that could enhance future screening protocols.

5.1.2 What is the problem to solve?

The issue lies in the lack of accurate and objective non-invasive imaging tools in melanoma diagnostics. If novel innovative imaging modalities addressing this gap were implemented in clinical practice, they could improve diagnostic accuracy, and support earlier and more precise clinical decision-making.

5.1.3 What is the importance of the topic?

The significance of this topic cannot be overstated, as melanoma remains a growing public health concern, with an estimated 325,000 new cases and nearly 57,000 deaths globally in 2020, and projections to 510,000 new cases and 96,000 deaths by 2040 (1). Early-stage detection is highly effective, yielding five-year survival rates above 95%, but this drops sharply to 20-40% when distant metastases are present, emphasizing the importance of timely diagnosis and intervention (2).

5.1.4 What would be the impact of our research results?

Our results could have a significant impact on dermatological practice by improving the early and accurate diagnosis of melanoma through the clinical implementation of novel, objective, and non-invasive imaging tools. Our findings support the development of more precise, reproducible, and accessible diagnostic pathways. This could reduce diagnostic delays, guide surgical planning, and ultimately improve patient outcomes and survival. Furthermore, the introduction of these methods may lower healthcare costs by minimizing unnecessary excisions and optimizing resource allocation in melanoma care.

5.2 Melanoma and Breslow thickness

Melanoma, a malignant tumor arising from melanocytes, is a major public health concern worldwide due to its aggressive nature, high mortality and high potential for metastasis. The occurrence of melanoma varies by population and region, with notably higher rates in areas of increased UV exposure (3), and is strongly associated with risk factors such as fair skin, frequent sunburns, excessive UV radiation, and familial predisposition (4, 5). The incidence of melanoma has been steadily rising over the past decades (6), emphasizing the necessity of timely intervention. Initiatives focusing on sun protection advocacy, routine skin screening, and early diagnosis play a pivotal role in melanoma epidemiology, highlighting prevention as a key strategy for reducing its incidence (7, 8). Current screening practices primarily rely on thorough skin examination, supported by visual inspection and dermoscopy. However, according to the American Academy of Dermatology (AAD), the National Institute of Health (NIH), and the National Comprehensive Cancer Network (NCCN), the final diagnosis of melanoma must always be confirmed by histopathological examination after surgical excision. Beyond determining the histological subtype of the melanoma, it is also necessary to assess Breslow thickness and the presence of ulceration, as these parameters form the basis of staging and guide appropriate treatment strategies (9, 10). Breslow thickness refers to the maximum depth of melanoma invasion measured in millimetres from the top of the granular layer to the deepest point of the tumor. It is the strongest independent prognostic factor for the clinical course of melanoma (9, 11) and also an essential part of melanoma staging, which recommends the appropriate surgical safety margin required for complete excision (Table 1) (12).

Table 1. Recommended surgical safety margins for melanoma excision (12)

Breslow thickness	Surgical safety margin*
In situ melanoma	0.5 cm^{+}
≤1.0 mm	1.0 cm
1.0-2.0 mm	1.0-2.0 cm
>2.0 mm	2.0 cm

** The safety margin should be measured from the edge of the lesion prior to surgery and may be adjusted depending on the anatomical location or to preserve function.*

$^{+}$ For lentigo maligna in situ melanoma, a 1 cm margin is recommended, especially for larger lesions located on the face.

Reoperation is necessary when the histologically determined Breslow thickness is greater than what was clinically expected, and the primary tumor was excised with an insufficient margin. Conversely, overestimating Breslow thickness can result in unnecessarily wide excisions, leading to larger scars and potential functional or aesthetic issues (especially in the head and neck region). Both scenarios place a burden on the healthcare system and patients (13, 14). Furthermore, Breslow thickness is the strongest predictor of the metastatic potential of melanoma and determines the indication for sentinel lymph node biopsy (SLNB). According to current guidelines, for patients with stage IB, T1b melanoma (Breslow depth <0.8 mm with ulceration or 0.8-1 mm with or without ulceration), or T1a lesions with Breslow depth >0.5 mm and other adverse features (age ≤42 years, head/neck location, lymphovascular invasion, and/or mitotic index ≥2/mm^2), performing SLNB should be strongly considered. For melanomas >1 mm in Breslow thickness, SLNB is routinely recommended, even in the absence of ulceration or other high-risk features (15). In the surgical management of melanoma, a two-step approach is applied, in which the initial excision is followed by a re-excision alongside SLNB after the histological Breslow thickness has been determined. Therefore, if we could have data on the tumor depth in advance, we could reduce the procedure to a single-step surgery combined with SLNB, thereby minimizing patient burden and expediting the staging process. By staging the melanoma earlier, we can promptly determine which imaging procedures are needed for follow-up and what therapeutic options will be needed going forward with the patient. Nowadays, oncodermatological research is actively exploring non-invasive imaging modalities for the early diagnosis of melanoma and the preoperative prediction of Breslow thickness, with the aim of reducing the tumor burden (16), as timely initiation of current therapeutic options can improve survival rates (17). However, melanoma still represents a significant diagnostic challenge due to its heterogeneity in clinical appearance and the limitations of available imaging techniques (18).

5.3 Limitations of current diagnostic procedures

Despite advances in awareness and prevention, early and accurate detection of melanoma remains a clinical challenge. Initial melanoma screening is predominantly based on visual inspection and dermoscopy. Dermoscopy is a non-invasive imaging technique that magnifies skin lesions, revealing fine morphological details not visible to the naked eye.

By utilizing specialized lights and filters, dermoscopy allows dermatologists to observe pigment patterns, structures, and vascular features crucial for diagnosing skin conditions (19, 20). Specific dermoscopic patterns and structures – such as irregular pigment networks, asymmetry, abrupt peripheral streaks, atypical vessels, regression structures, and uneven colour distribution – aid in distinguishing benign from malignant lesions, particularly in suspected melanoma cases (21). Over the past decades, dermoscopy has become an invaluable non-invasive tool in dermatology, widely integrated into routine clinical practice for the evaluation of pigmented and non-pigmented skin lesions. However, despite its widespread use, dermoscopy remains highly operator-dependent and often lacks the objectivity needed for consistent assessment. Its effective application requires specialized knowledge and substantial experience, as accurate interpretation depends on a thorough understanding of dermoscopic structures. Furthermore, the observed features are often nonspecific, meaning that lesions of different origins display similar patterns, making diagnostic accuracy heavily reliant on the examiner's expertise. Additionally, dermoscopy is not suitable for accurately determining the depth of tumor invasion; it only allows for an approximate estimation, which is insufficient for developing an appropriate therapeutic plan in cases of melanoma (22). Pathological staging of melanoma depends on histology and serves as a crucial component of the diagnostic pathway. The histological evaluation provides detailed insights into key tumor characteristics, including architectural patterns, cellular morphology, mitotic activity, and Breslow thickness. These parameters are essential for precise staging, guiding clinical decision-making, and selecting the most appropriate therapeutic strategy for patients (23-25). Therefore, the gold standard for the diagnosis of melanoma is histopathology (26), although it is an invasive procedure and does not provide prompt results. Consequently, there is an unmet need for non-invasive, objective imaging tools that can aid in the early detection and preoperative assessment of melanoma.

5.4 Novel optical imaging modalities

Advances in technology have led to the development of novel non-invasive optical imaging techniques for the detection of melanoma (17). The advantage of these diagnostic methods compared to conventional dermoscopy is that they may offer higher resolution images of the skin, and they often provide reproducible quantitative measurements (27).

These instruments are based on different biophysical principles, including cameras working with the properties of light and tissues to capture and analyze images at multiple wavelengths (e.g., multispectral imaging); analytical techniques that provide information on the molecular composition, structure, and dynamics based on the scattering of photons by molecular vibrations (e.g., Raman spectroscopy); confocal imaging techniques based on light-tissue interaction (e.g., reflectance confocal microscopy); devices operating with light interference to visualize tissue microstructures (e.g., optical coherence tomography) and fluorescence methods (e.g., dermatofluoroscopy) (28). Teledermoscopy is an emerging diagnostic tool for the prevention and diagnosis of skin diseases when face-to-face visualization of lesions is difficult (29). The evaluation and diagnosis of the obtained images can also be assisted using artificial intelligence (e.g., dermoscopy combined with artificial intelligence and multispectral imaging combined with artificial intelligence), thereby increasing diagnostic efficacy, consistency and reducing interobserver variability. High-frequency ultrasound (HFUS), also known as high-resolution ultrasound, employs sound waves with frequencies greater than 20 MHz to generate images of the tissue structures (30). Melanoma is generally characterized by hypoechogenic, homogenous, and well-defined lesions on ultrasound images (31). Recent advances in handheld HFUS devices have integrated an optical module to facilitate precise localization of the ultrasound beam, enabling accurate cross-sectional image positioning. Using HFUS, the depth of the melanoma can be measured by determining the distance between the top layer of the skin and the deepest point of the tumor. Therefore, HFUS may be capable of preoperative diagnosis of melanoma (32) and estimation of Breslow thickness (31). All these techniques show promise in improving diagnostic accuracy by providing high-resolution, real-time, non-invasive visualization of lesion morphology and depth. However, their clinical utility is often limited by high costs, the need for specialized training, and limited penetration depth. While these modalities can be applied alongside current diagnostic techniques, the question of whether a single imaging tool could serve as the optimal solution for melanoma diagnosis and preoperative assessment of Breslow thickness remains unresolved.

6 OBJECTIVES

6.1 Study I. – Comparing the efficacy of novel OG-HFUS and MSI in preoperative estimation of Breslow thickness

The aim of this study was to compare the diagnostic accuracy of OG-HFUS and MSI for preoperative estimation of Breslow tumor thickness in primary melanoma. Although both novel handheld devices offer a new perspective on non-invasive assessment of tumor depth, their relative performance in clinical settings has not yet been evaluated. In a prospective clinical study, we applied each modality to a cohort of 101 melanoma patients and compared their Breslow thickness estimates against the gold-standard histology to determine which imaging method provides greater accuracy for preoperative decision-making in melanoma care.

6.2 Study II. – Comparing the diagnostic accuracy of novel non-invasive optical imaging techniques for melanoma diagnosis

The objective of this study was to perform a comprehensive systematic review and meta-analysis evaluating the diagnostic performance of all optical imaging methods for melanoma detection. Although numerous new imaging modalities have been introduced in dermatology in recent years, the performance of these technologies (particularly in clinical applications) has not yet been compared. This meta-analysis aimed to clarify and compare the diagnostic accuracy of each optical imaging technique and provide evidence-based insights to guide clinical decision-making and future research priorities in melanoma diagnostics.

7 METHODS

7.1 Study I.

7.1.1 Study design and setting

The research was conducted as a single-center, prospective validation study at the Department of Dermatology, Venereology, and Dermatooncology, Semmelweis University. We enrolled 101 consecutive adult patients (≥18 years) who had a suspected primary cutaneous melanoma scheduled for surgical excision. Informed consent was obtained from all subjects involved in the study. Before the operation, each participant underwent non-invasive imaging with two handheld devices (MSI and OG-HFUS) in a standardized sequence. Imaging was performed by trained operators who were blinded to the histopathologic results at the time of measurement. Following imaging, all lesions were excised. Patients whose final histopathological diagnosis was not primary melanoma were excluded from the study. For those histologically confirmed as melanoma, Breslow thickness was determined on sections by expert dermatopathologists (reference standard). The primary endpoint was to compare the agreement between each modality's Breslow thickness estimates and the histologic depth measurements. The study was conducted according to the guidelines of the Declaration of Helsinki and approved by the Institutional Ethics Committee of Semmelweis University (SE RKEB no. 16/2022).

7.1.2 Inclusion and exclusion criteria

The inclusion criteria required obtaining informed consent from patients and confirming primary cutaneous melanoma through histopathological evaluation by expert dermatopathologists. Eligibility was limited to melanomas with a Breslow thickness of less than 10 mm. Exclusion criteria included *in situ* or metastatic melanomas, primary melanomas located in specific anatomical sites (such as acral areas, the genital region, or mucosal surfaces), where the imaging procedure was challenging. Additionally, lesions characterized by extensive hair, bleeding, or scaling that could impair accurate imaging were also excluded.

7.1.3 OG-HFUS imaging protocol

All scans were performed at the Department of Dermatology, Venereology, and Dermatooncology, Semmelweis University, using the portable Dermus SkinScanner device (Dermus Ltd., Budapest, Hungary). This handheld OG-HFUS system integrates a single-element ultrasound transducer (operating at a nominal center frequency of 33 MHz ranging with a 20-40 MHz bandwidth) with an optical imaging module for precise lesion positioning. A silicone membrane covers the imaging window, and standard ultrasound gel is applied before each acquisition. The dermoscopy-based optical window provides a 15×15 mm field of view, while the ultrasound extends laterally up to 12 mm and penetrates to a maximum depth of 10 mm. When a lesion exceeded the optical field, we acquired additional image sets to ensure full coverage and analysis. Both the optical and ultrasound images are then stored using a secure cloud-based system, which saves all the photos under a patient ID with the birth date, sex, diagnosis, and exact location of the body region (33). Ultrasound images are displayed in a colour-scale format to enhance contrast. The presumed tumor thickness was measured from these ultrasound images within one minute of acquisition.

7.1.4 MSI imaging protocol

All multispectral imaging was performed at the Department of Dermatology, Venereology, and Dermatooncology, Semmelweis University, using a handheld prototype co-developed by the University of Latvia and Riga Technical University. The illumination module consisted of a ring comprising four types of LED diodes emitting at wavelengths of 405 nm (for autofluorescence/AF excitation), 525 nm (for green/G excitation), 660 nm (for red/R excitation), and 940 nm (for infrared/IR excitation), enabling penetration into different skin layers. The device was designed to capture skin diffuse reflectance images using the fixed circular arrangement of these four LED diodes. For quantitative analysis, we utilized the G, R, and IR channels. The LEDs provided an irradiating power density of 20 mW/cm^2 and had a field of view of 2×2 cm^2. In cases where the lesion size exceeded the camera's field of view, we captured additional image sets to ensure comprehensive coverage and analysis. The LEDs are mounted at a fixed 35 mm radius and fitted with a matte diffuser for uniform skin illumination. Image acquisition was performed using a 5-megapixel colour CMOS IDS camera (MT9P006STC, IDS uEye UI3581LE-C-HQ,

Obersulm, Germany) positioned 60 mm from the illuminated skin. To capture the AF emission images and block the 405 nm excitation illumination, a long-pass filter (T515 nm >90%) was placed in front of the camera (34, 35). A black marker was applied next to the lesions to align and scale the different spectral channel images prior to quantitative analysis (36). The acquired images were automatically transferred to a cloud server for further data processing and analysis (37). Multispectral images were analyzed using ImageJ v1.46 software (NIH, Bethesda, MD, USA) (38). For intensity analysis and shape description, freehand regions of interest (ROIs) were drawn around each lesion in the G, R, and IR channels and managed via the ROI Manager to ensure identical sampling areas across wavelengths. We extracted mean gray value (integrated density/area), circularity ($4\pi \cdot \text{area}/\text{perimeter}^2$), solidity (area/convex area), and roundness ($4 \cdot \text{area}/(\pi \cdot \text{major axis}^2)$) as defined in our previous work when we developed the melanoma classification algorithm (39). The entire imaging procedure and subsequent thickness estimation can be performed within minutes.

7.1.5 Melanoma classification algorithm

In our previous research (39), we developed an MSI-based algorithm that uses shape descriptors and intensity metrics to classify melanomas into three clinically relevant subgroups (Breslow thickness <1 mm, Breslow thickness between 1-2 mm, and Breslow thickness >2 mm). In the present study, we applied this modified classification algorithm (Figure 1) to assess MSI performance. The first step of the original algorithm was not used in this research. Lesions are first divided by circularity at a 0.75 A.U. threshold (low-circularity and high-circularity). The low-circularity branch melanomas are then split by G-channel intensity at 8.0 A.U. threshold, and the high-circularity branch melanomas are split by IR-channel intensity at 113.7 A.U. threshold. The lesions under the threshold of circularity and over the threshold of G-channel intensity are classified as Breslow <1 mm, whereas lesions with also low-circularity and under the threshold of G-channel intensity are classified as Breslow between 1-2 mm. The high-circularity melanomas with lower IR-channel intensity were classified as Breslow >2 mm, and melanomas with higher IR-channel intensity were classified as Breslow between 1-2 mm.

7.1.6 Statistical analysis

To assess the accuracy of OG-HFUS, we compared our depth measurements on the captured ultrasound images with histologically verified Breslow thickness values using Pearson's correlation and evaluated reliability within each Breslow thickness category. For MSI, we performed multivariate correlation analysis, where we developed a multivariate linear regression model that combined lesion circularity and spectral intensity features (using green, red, and infrared channels) to estimate Breslow thickness. We then quantified the strength of this association by calculating the Pearson correlation between the model's predicted depths and the histologically confirmed Breslow measurements. Significance evaluation was conducted using F-statistics. For statistical evaluation, we used the *scikit-learn*, *scipy*, and *statmodels* libraries in the Python programming language and environment. For each clinical category, we computed sensitivity, specificity, positive predictive value (PPV), negative predictive value (NPV), and mean squared error (MSE). For overall model estimation, we presented the micro-averaged sensitivity, specificity, PPV, and NPV. Concordance was quantified using Cohen's kappa (κ), and statistical significance was defined as $p<0.05$. Results are presented as mean +/− standard deviation (SD).

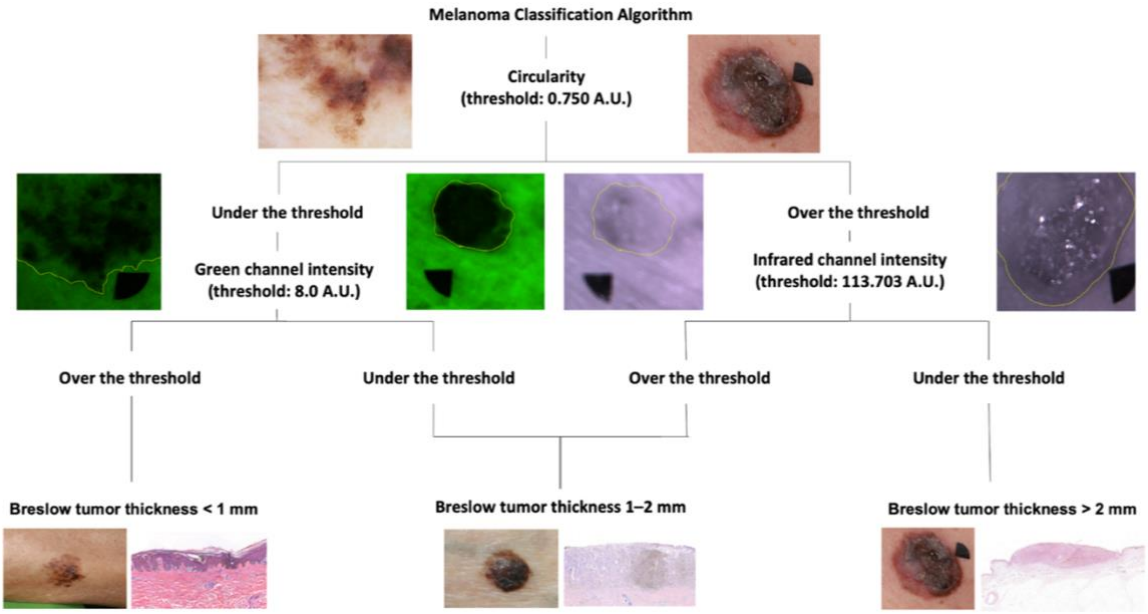

Figure 1. Melanoma classification algorithm (39)

7.2 Study II.

7.2.1 Search strategy

We conducted a systematic literature review and meta-analysis following the latest guidelines of the Cochrane Handbook (40). The study protocol was prospectively registered on the PROSPERO International Prospective Register of Systematic Reviews (registration number CRD42023480274). We did not deviate from the protocol. We documented our systematic review and meta-analysis based on the guidance of the PRISMA (Preferred Reporting Items for Systematic Reviews and Meta-Analyses) 2020 Statement (41). The search was systematically carried out in three extensive scientific databases: MEDLINE (via PubMed), CENTRAL (Cochrane Central Register of Controlled Trials), and Embase (by Elsevier) from inception to November 15, 2023. The search terms included three key elements: (I) terms related to melanoma, (II) terms related to diagnosis, and (III) a list of all optical imaging techniques. We used this predefined search key in all databases without any filters or restrictions: melanom* AND (diagnos* OR detect*) AND (dermoscop* OR dermatoscop* OR fluorometr* OR fluorimetr* OR spectrofluorometr* OR spectrofluorimetr* OR dermatofluoroscop* OR polarimetr* OR ((“optical” OR “hyperspectral” OR “multispectral” OR “spectral” OR spectroscop* OR fluoresc* OR multiphoton* OR multi-photon* OR “two-photon” OR polar* OR “Mueller” OR “terahertz” OR “photoacoustic”) AND “imaging”) OR ((epiluminesc* OR “incident light” OR “surface” OR “confocal” OR “laser scanning” OR fluoresc* OR “Raman” OR “nonlinear” OR “non-linear” OR multiphoton* OR multi-photon* OR “two-photon”) AND microscop*) OR ((“optical coherence” OR multiphoton* OR multi-photon* OR “photoacoustic”) AND tomograph*) OR ((“optical” OR “Raman” OR reflect* OR “remission” OR fluoresc*) AND (spectroscop* OR spectrometr*)) OR ((“multispectral” OR “spectrum”) AND “analysis”) OR ((“laser” OR “two-photon”) AND fluoresc*) OR ((“Stokes” OR “Mueller”) AND polarimetr*) OR ((“self-mixing” OR “optical feedback”) AND interferometr*) OR (“Raman” AND scatter*) OR (“harmonic” AND “generation”). In addition, we examined the bibliography of the eligible articles.

7.2.2 Study selection and eligibility criteria

The inclusion criteria encompassed any peer-reviewed studies that met the following Population – Index test – Reference test – Diagnosis (PIRD) framework: (P) patients suspected of having melanoma were examined using (I) non-invasive optical diagnostic methods, then the results were compared with (R) histopathology, and the final diagnosis became (D) melanoma. The primary outcome was the diagnostic accuracy of non-invasive optical imaging techniques for detecting melanoma. There were no restrictions based on age, sex, or ethnicity regarding the study population in the selected articles. Studies were excluded if we could not extract meaningful data from them, or if they involved fewer than five melanoma cases, as well as case reports, meta-analyses, systematic reviews, and letters. After removing duplicates using the reference management software EndNote 20 (Clarivate Analytics, Philadelphia, PA, USA), two review authors independently assessed titles, abstracts, and full texts according to the predefined eligibility criteria for selection. We calculated Cohen's kappa coefficient after each selection process to measure interrater reliability (42). A third review author was responsible for resolving any conflicts that arose.

7.2.3 Data extraction

Data from eligible studies were extracted by two independent review authors using a standardized data collection form. A third independent author was responsible for resolving any disagreements. The following data were extracted with a standardized collection method to a Microsoft Excel sheet (Office 365, Microsoft, Redmond, WA, USA): first author, publication year, digital object identifier (DOI) number, study design, study period, location, number of study centers, count of pigmented lesions, number of histologically verified melanomas, index test, reference standard, as well as details about the patients such as number, age, and gender distribution. Additionally, the data covered Breslow thickness, true positive, false negative, false positive, true negative cases, sensitivity, specificity, PPV, NPV, diagnostic accuracy, and area under the curve (AUC) values. Where available, sensitivity and specificity values were extracted directly. In cases where these values were not reported, they were calculated from the remaining data.

7.2.4 Quality assessment

Risk of Bias assessment

The risk of bias was assessed based on the recommendation of the Cochrane Collaboration (40). For diagnostic questions, we used the QUADAS-2 (Quality Assessment of Diagnostic Accuracy Studies included in the Systematic Reviews) tool (43). In each study, we analyzed the risk of bias for every imaging technique separately. Two independent reviewers conducted the quality assessment of the outcomes, and an independent third investigator resolved the disagreements. Publication bias was evaluated through visual inspection of funnel plots.

GRADE assessment

We assessed the quality of evidence in the included studies using the Grading of Recommendations Assessment, Development and Evaluation (GRADE) approach (44), with the GRADEpro GDT software (GRADEpro GDT: GRADEpro Guideline Development Tool. McMaster University and Evidence Prime, 2024, available from gradepro.org). Outcomes were rated as high, moderate, low, or very low quality of evidence.

7.2.5 Data synthesis and statistical analysis

For the estimation of pooled specificity and sensitivity, the bivariate model of Chu et al.(45) and Reitsma et al.(46) was fitted. This approach considers the possible association between sensitivity and specificity. We plotted individual and pooled sensitivities and specificities of the studies included, their summary estimates, and the corresponding 95% confidence and prediction regions. In these visualizations, the size of the ellipsoids reflects the weight of the studies calculated according to the method described by Burke et al.(47). The PPV and NPV results were calculated from the estimated specificity and sensitivity values at a melanoma prevalence rate of 30%, as this became the average prevalence value from the studies examining melanoma suspicious lesions. We also calculated the diagnostic odds ratio (DOR) with its 95% confidence interval (CI), a single indicator that combines the sensitivity and specificity of a diagnostic test, thus simplifying the comparison of test performance. It is defined as the ratio of the odds of a positive test

result for individuals with the disease compared to the odds of a positive test result for individuals without the disease. The DOR ranges from 0 to infinity, with higher values indicating better performance (48). Heterogeneity was assessed by calculating the I^2 measure and its CI arising from the separate univariate analyses. Statistical analyses were performed using R statistical software (version 4.1.2., R Core Team (2023). R: A language and environment for statistical computing. R Foundation for Statistical Computing, Vienna, Austria, https://www.R-project.org/) using the meta (49) and the lme4 (50) packages and were partially based on the web-tool of Freeman et al.(51). The statistical analyses followed the advice of Harrer et al.(52).

8 RESULTS

8.1 Study I: Prospective diagnostic accuracy study

8.1.1 Characteristics of the study population

A total of 101 patients with primary cutaneous melanoma were enrolled, characterized by a mean age of 64.20 ± 15.24 years, comprising 53 males and 48 females, resulting in a sex ratio of 52.5% and 47.5%, respectively. Lesion locations included the trunk (n = 60), extremities (n = 32), cheek (n = 6), forehead (n = 2), and neck (n = 1). The average histologic Breslow thickness was 1.61 mm ± 1.69 mm, with values ranging from a minimum thickness of 0.135 mm to a maximum of 8.12 mm. The detailed breakdown of melanoma subtypes is shown in Table 2.

Table 2. Melanoma subtype distribution

Subtype	Lesion (*n*)	Distribution Ratio (%)
SSM	69	68.32
NM	8	7.92
SSM sec. nod.	10	9.90
LMM sec. nod.	1	0.99
LMM	6	5.94
ALM	1	0.99
UC	4	3.96
Naevoid	2	1.98

Abbreviations: *SSM - Superficial spreading melanoma; NM - Nodular melanoma; SSM sec. nod. - Superficial spreading melanoma with secondary nodular component; LMM sec. nod. - Lentigo maligna melanoma with secondary nodular component; LMM - Lentigo maligna melanoma; ALM - Acral lentiginous melanoma; UC - Unclassified melanoma*

8.1.2 Diagnostic performance of OG-HFUS

The integrated optical and HFUS imaging procedure is illustrated in Figure 2. The overall performance of OG-HFUS demonstrated substantial reliability, with a high Cohen's kappa coefficient (κ = 0.858 [0.763;0.952]). This indicates almost perfect agreement between OG-HFUS imaging and the histologic Breslow thickness measurements. This finding is further supported by Pearson correlation analysis (Figure 4), which demonstrated a significant positive correlation between OG-HFUS measurements and histological Breslow thickness (r = 0.943, $p<0.0001$). OG-HFUS achieved its highest diagnostic accuracy in the Breslow <1 mm subgroup (κ = 0.937 [0.867;1.000], almost perfect agreement), while its lowest accuracy occurred in the Breslow between 1-2 mm subgroup (κ = 0.701 [0.503;0.900], substantial agreement). The complete summary of OG-HFUS performance metrics stratified by Breslow depth is given in Table 3.

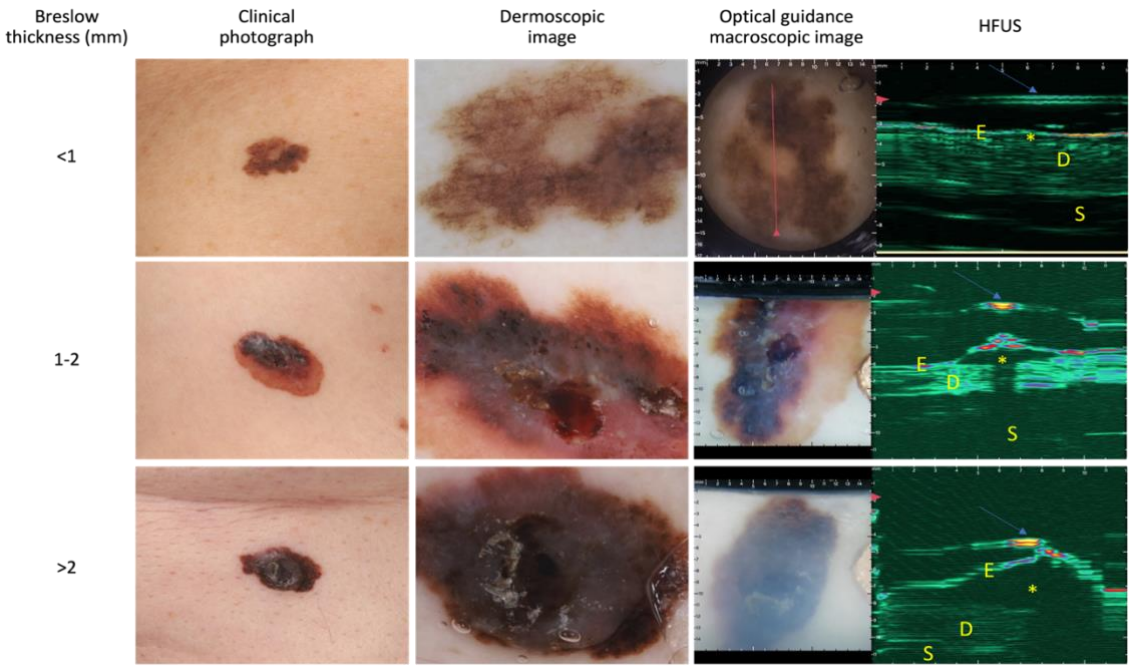

Figure 2. Clinical, dermoscopic, optical and HFUS images of distinct melanoma lesions stratified by OG-HFUS into three subgroups based on Breslow thickness: <1 mm (row 1), 1-2 mm (row 2), and >2 mm (row 3). On the HFUS images, yellow asterisks (*) represent the tumor, red arrows on the left indicate the membrane, and the yellow letters stand for E: epidermis, D: dermis, S: subcutis.

8.1.3 Diagnostic performance of MSI

The MSI images acquired in the different spectral channels are shown in Figure 3. The overall performance of MSI demonstrated fair agreement, as Cohen's kappa coefficient became low (κ = 0.440 [0.298;0.583]). This corresponds to only a fair level of concordance between MSI and histologic Breslow measurements. Individually, among the shape descriptors and intensity values of different channels, the IR channel showed the strongest correlation (r = −0.659, p<0.0001) with Breslow thickness. In contrast, the multivariate linear model incorporating shape descriptors and spectral intensities achieved a higher overall correlation (r = 0.714, p<0.0001) (Figure 5), though this still underperforms compared to OG-HFUS. MSI achieved its highest diagnostic accuracy in the Breslow >2 mm subgroup (κ = 0.680 [0.517;0.842], substantial agreement), while its lowest accuracy was in the Breslow between 1-2 mm subgroup (κ = 0.177 [-0.052;0.406], fair agreement). The detailed MSI performance metrics for estimating Breslow thickness are summarized in Table 4.

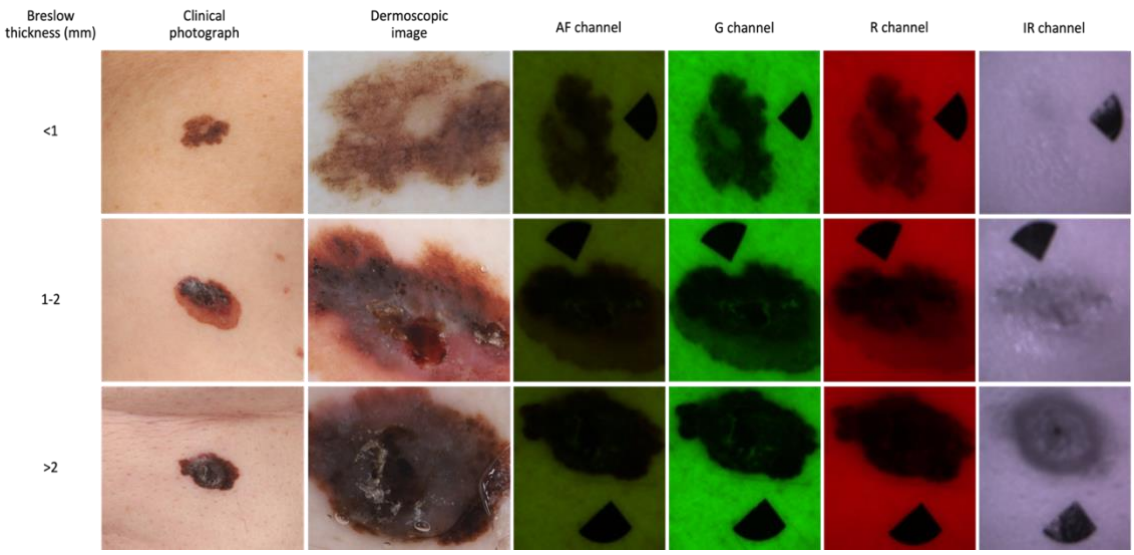

Figure 3. Clinical, dermoscopic and multispectral images (in the AF, G, R, and IR channels) of distinct melanoma lesions stratified by MSI into three subgroups based on Breslow thickness: <1 mm (row 1), 1-2 mm (row 2), and >2 mm (row 3). On the different spectral images, black markers placed next to the lesions serve as fixed reference points to improve image alignment (36).

8.1.4 Comparative analysis

In our comparative analysis, OG-HFUS demonstrated superior diagnostic accuracy in the preoperative estimation of Breslow thickness against MSI. OG-HFUS achieved a pooled sensitivity of 91.8%, a pooled specificity of 96.0%, and exhibited almost perfect agreement for the Cohen's kappa coefficient (κ = 0.858 [0.763;0.952]). In contrast, MSI showed an overall sensitivity of 62.6% and an overall specificity of 81.3%, with a fair agreement (κ = 0.440 [0.298;0.583]). OG-HFUS also displayed a PPV of 91.8% and an NPV of 96.0%, surpassing the PPV (62.6%) and NPV (81.3%) of MSI. However, not only in the overall results, but also across all Breslow categories, OG-HFUS yielded lower MSE, and higher sensitivity, specificity, predictive values, and Cohen's kappa compared to MSI (see Tables 3 and 4). These findings underscore the improved diagnostic accuracy and efficacy of the OG-HFUS approach in preoperative determination of Breslow thickness when compared with MSI.

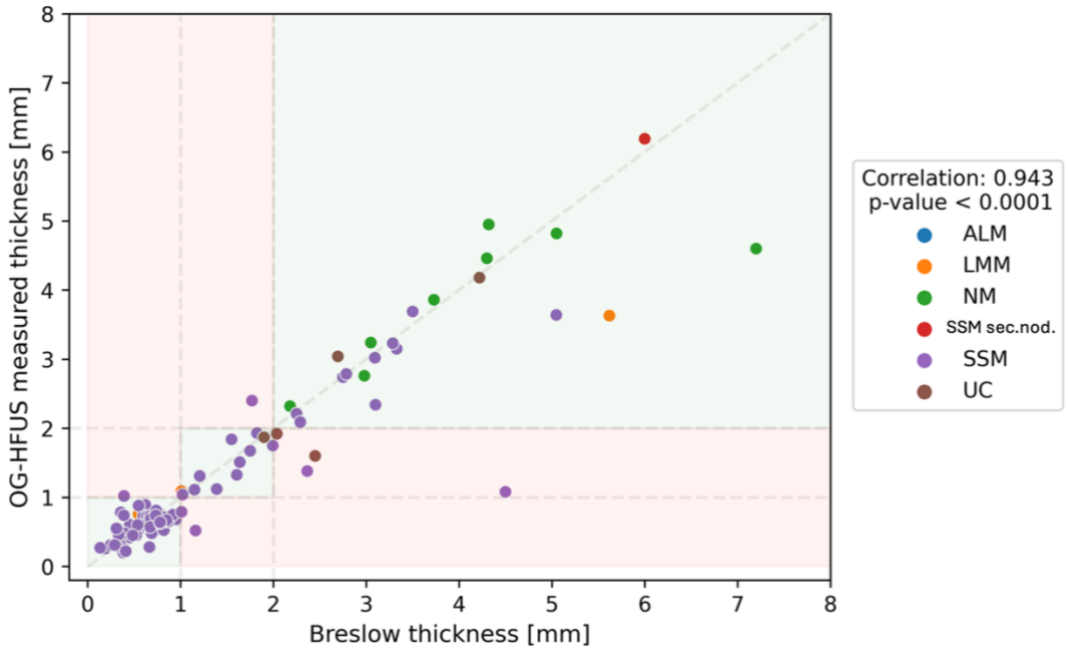

Figure 4. Pearson correlation analysis between OG-HFUS measured thickness (y-axis) and histologically confirmed Breslow thickness (x-axis). Each data point on the graph is colour-coded by one melanoma subtype.

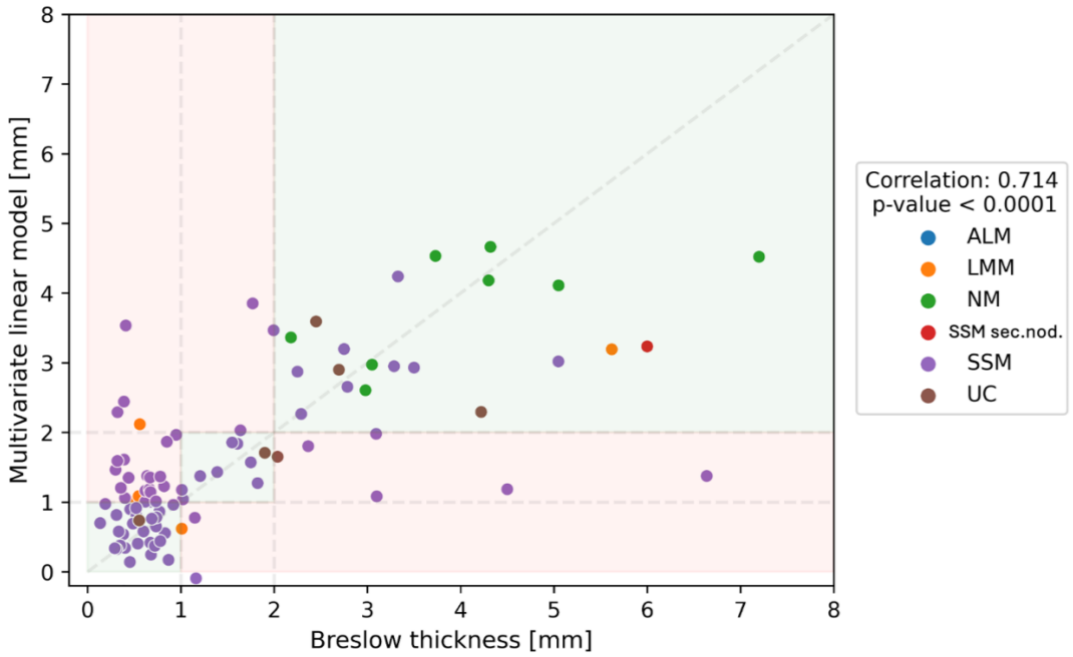

Figure 5. Pearson correlation analysis between MSI measured thickness (y-axis) and histologically confirmed Breslow thickness (x-axis). Each data point on the graph is colour-coded by one melanoma subtype.

Table 3. Diagnostic accuracy of OG-HFUS for estimating Breslow thickness

Breslow (mm)	**Patients (*n*)**	**MSE**	**Sensitivity (%)**	**Specificity (%)**	**PPV (%)**	**NPV (%)**	**Cohen's Kappa (κ)**	**95% CI**
<1	56	0.034	98.2	95.2	96.5	97.6	0.937	0.867-1.000
1-2	15	0.080	80.0	94.0	70.6	96.3	0.701	0.503-0.900
>2	27	1.02	85.2	98.6	95.8	94.6	0.868	0.755-0.980
Total	98	0.31	91.8	96.0	91.8	96.0	0.858	0.763-0.952

Abbreviations: *MSE - Mean squared error; PPV - Positive predictive value; NPV - Negative predictive value; CI - Confidence interval*

Table 4. Diagnostic accuracy of MSI for estimating Breslow thickness

Breslow (mm)	Patients (*n*)	MSE	Sensitivity (%)	Specificity (%)	PPV (%)	NPV (%)	Cohen's Kappa (κ)	95% CI
<1	56	0.64	55.4	93.0	91.2	61.5	0.457	0.286-0.627
1-2	15	0.61	60.0	67.9	25.0	90.5	0.177	-0.052-0.406
>2	28	3.36	78.6	90.1	75.9	91.4	0.680	0.517-0.842
Total	99	1.41	62.6	81.3	62.6	81.3	0.440	0.298-0.583

Abbreviations: *MSE - Mean squared error; PPV - Positive predictive value; NPV - Negative predictive value; CI - Confidence interval*

8.2 Study II: Systematic review and meta-analysis

8.2.1 Search and Selection

The PRISMA flowchart (41) is illustrated in Figure 6. We initially identified 16,239 records through database searching, of which 136 studies (53-188) were found eligible. Additionally, via citation searching, we found 5 more eligible studies (189-193). Overall, 141 articles were included in the qualitative analysis (systematic review), of which 138 studies were included in the quantitative synthesis (meta-analysis).

8.2.2 Basic characteristics of included studies

The baseline characteristics table (Table S2 in the Supplementary material of the article) provides a comprehensive overview of the studies included in the systematic review. It summarizes key attributes such as publication data, study design, location, and period, as well as detailed sample information including the number of patients and lesions, the number and proportion of histologically verified melanomas, and demographic data like age and gender distribution. In the index test column of the table, we first listed the investigated optical imaging modality, followed in parentheses by the specific device or algorithm used in the diagnostic assessment of the study. This structured presentation facilitates comparison across studies and highlights the diversity in geographic settings, study designs, and patient populations, which are crucial for interpreting the generalizability and applicability of the findings. The most common study designs among the included articles were prospective single-center or multicenter studies. In terms of the data collection period, the included studies encompassed an overall timeframe between 1989 and 2022. We included diagnostic accuracy studies from around the world, and the specific geographic locations are indicated in the baseline table.

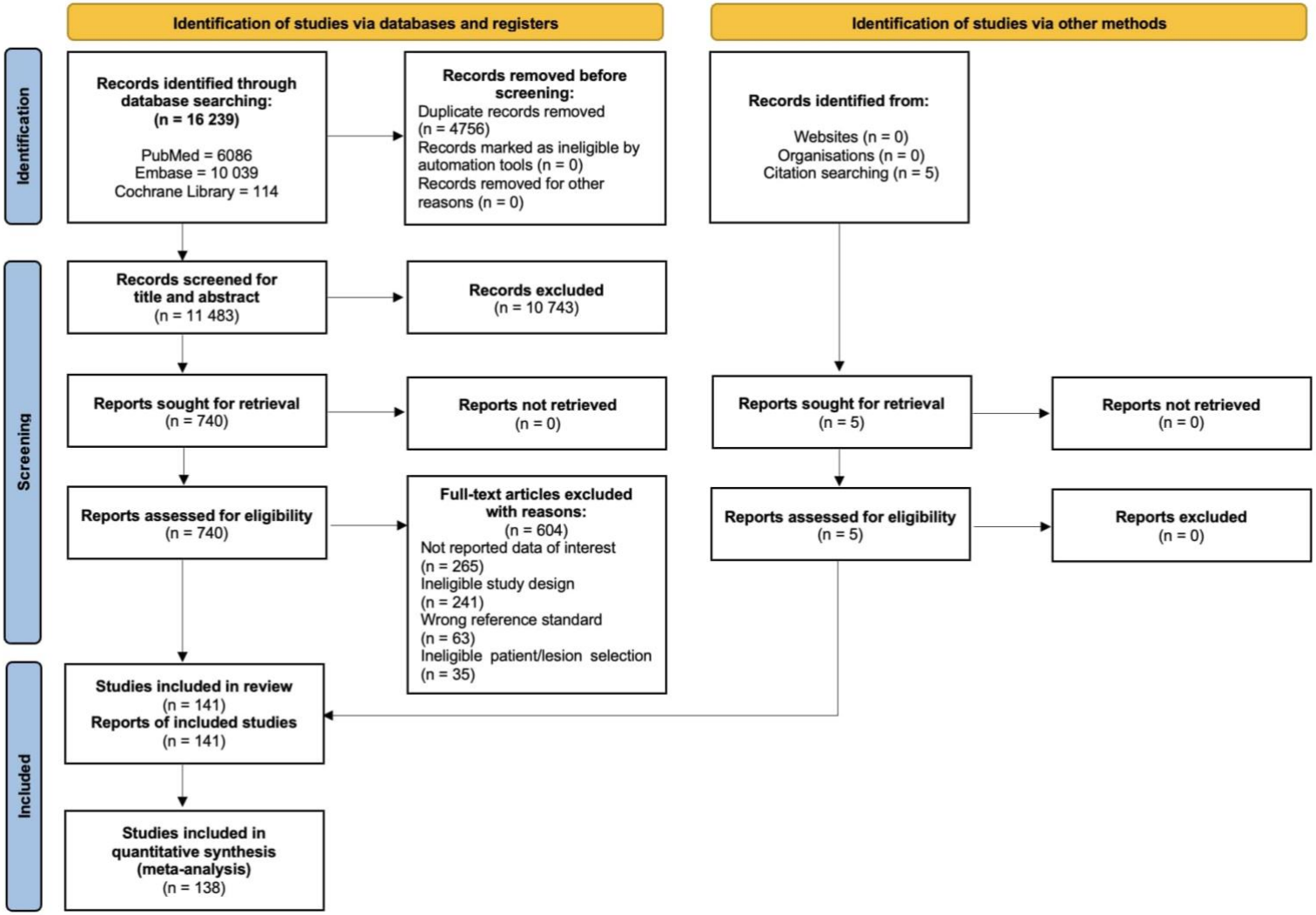

Figure 6. PRISMA 2020 flowchart representing the study selection process (41)

8.2.3 Quantitative analysis (meta-analysis)

The bivariate analyses revealed that various optical imaging techniques displayed different levels of sensitivity and specificity (Figure 7). Among the assessed methods, both DSC+AI and RCM achieved the highest sensitivity (0.93 [0.88; 0.96] and 0.93 [0.9282; 0.9293], respectively). Nevertheless, DSC+AI demonstrated a slightly superior specificity (0.77 [0.70; 0.83]) compared to RCM (0.749 [0.7475; 0.7504]). Furthermore, MSI+AI also exhibited high sensitivity (0.92 [0.82; 0.97]) along with a comparatively high specificity (0.80 [0.67; 0.89]). The specificities for standalone DSC and TeleDSC were similar (0.82 [0.78; 0.86] and 0.85 [0.73; 0.92]), although DSC had greater sensitivity (0.87 [0.84; 0.90]) than TeleDSC (0.84 [0.70; 0.92]). Standalone MSI exhibited lower specificity (0.64 [0.49; 0.77]) but maintained a high sensitivity (0.87 [0.78; 0.92]). The results of these individual summary receiver operating characteristics (sROC) curves, aggregated into a bivariate random-effects model, which is illustrated in Figure 8. Different colours are used to distinguish between the optical imaging modalities. The position of the dots and the size of the ellipses give the opportunity to visually compare the diagnostic accuracy and reliability of each method. All individual Forest plots detailing the pooled sensitivity and specificity outcomes for these optical imaging methods can be found in the Supplementary material of our article (see Figures S1-S12).

In addition to the previously mentioned six methods, we investigated three other optical imaging techniques: dermatofluoroscopy (DF), optical coherence tomography (OCT), and Raman spectroscopy (RS). Due to the limited number of available studies, we were only able to perform univariate analyses on them. Therefore, their sensitivity and specificity results are presented in Forest plots rather than sROC curves. The detailed Forest plots illustrating the sensitivity and specificity of these three imaging modalities can be found in Figures 9-14.

Table 5 summarizes the sensitivity, specificity, PPV, NPV, DOR, and corresponding certainty of evidence for all the optical diagnostic tools investigated in the meta-analysis. DSC+AI, RCM, and MSI+AI achieved the highest NPV values (0.96). OCT and TeleDSC reached the highest PPV values (0.71). Overall, OCT demonstrated the highest DOR (64.25 [0.25; 16391.97]) and nearly similar sensitivity (0.84 [0.72; 0.96]) and specificity

(0.85 [0.63; 1.00]) results. RCM showed a high level of evidence for sensitivity (0.93 [0.928; 0.93]) and a moderate level of evidence for specificity (0.75 [0.748; 0.75]). Combining AI with imaging modalities such as DSC and MSI generally improved diagnostic performance (DOR of DSC from 27.32 [19.54; 38.20] to 32.62 [17.74; 59.97] and DOR of MSI from 9.62 [4.80; 19.28] to 37.51 [10.16; 138.51]). DSC, TeleDSC, and RS showed moderate to low diagnostic performance (DOR of DSC 27.32 [19.54; 38.20], DOR of TeleDSC 24.00 [4.88; 118.04], DOR of RS 22.66 [0.81; 631.00]). DF, despite its high sensitivity (0.91 [0.88; 0.95]), had the lowest specificity (0.55 [0.37; 0.74]) of the methods evaluated and showed very low evidence levels in both cases. Figures 15-23 display the individual Forest plots of DOR for each optical method.

8.2.4 Qualitative analysis (systematic review)

Table 6 summarizes the performance of three non-invasive optical modalities - near-infrared and skin impedance (NIR-SI) spectroscopy, multimodal spectral diagnosis (MSD), and multiphoton microscopy (MPM) - solely included in the systematic review. In a 2013 study by Bodén et al., NIR-SI spectroscopy (192) was performed with a Bruker Matrix F spectrometer on 50 lesions (10 true positives, 2 false negatives, 2 false positives, 36 true negatives). The technique achieved high specificity (0.95) and sensitivity (0.83). Lim and colleagues (2014) combined Raman spectroscopy, diffuse optical spectroscopy, and laser-induced fluorescence spectroscopy to assess 29 lesions, reporting perfect separation between malignant and benign cases (12 true positives, 0 false negatives, 0 false positives, 17 true negatives). MSD (128) achieved perfect sensitivity and specificity at 1.00. Dimitrov et al. (2009) evaluated MPM (93) (using DermaInspect) across 52.5 lesions (19.5 true positives, 6.5 false negatives, 5.4 false positives, 21.6 true negatives). The resulting sensitivity (0.75 [0.57; 0.93]) and specificity (0.80 [0.67; 0.93]) were moderate.

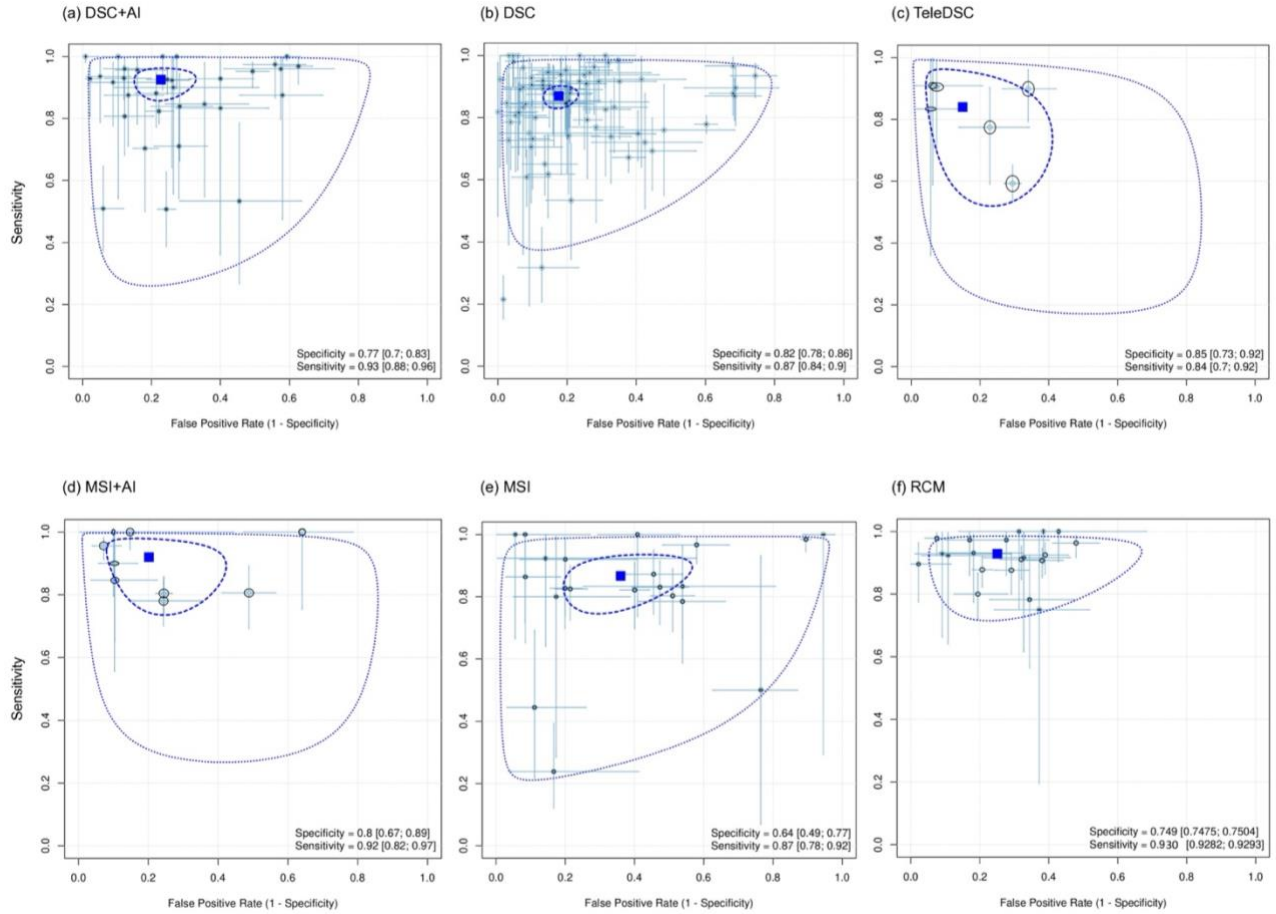

Figure 7. Bivariate plots of the articles evaluating the diagnostic accuracy of (a) DSC+AI, (b) DSC, (c) TeleDSC, (d) MSI+AI, (e) MSI, and (f) RCM. On each figure, the individual study estimates are black circles, and their confidence intervals are blue error bars. The summary points (blue square) represent the pooled sensitivity and specificity results with 95% confidence regions (dashed blue ellipse) and sROC curves (dotted blue line). The pooled specificity and sensitivity values are reported in the bottom right corners.

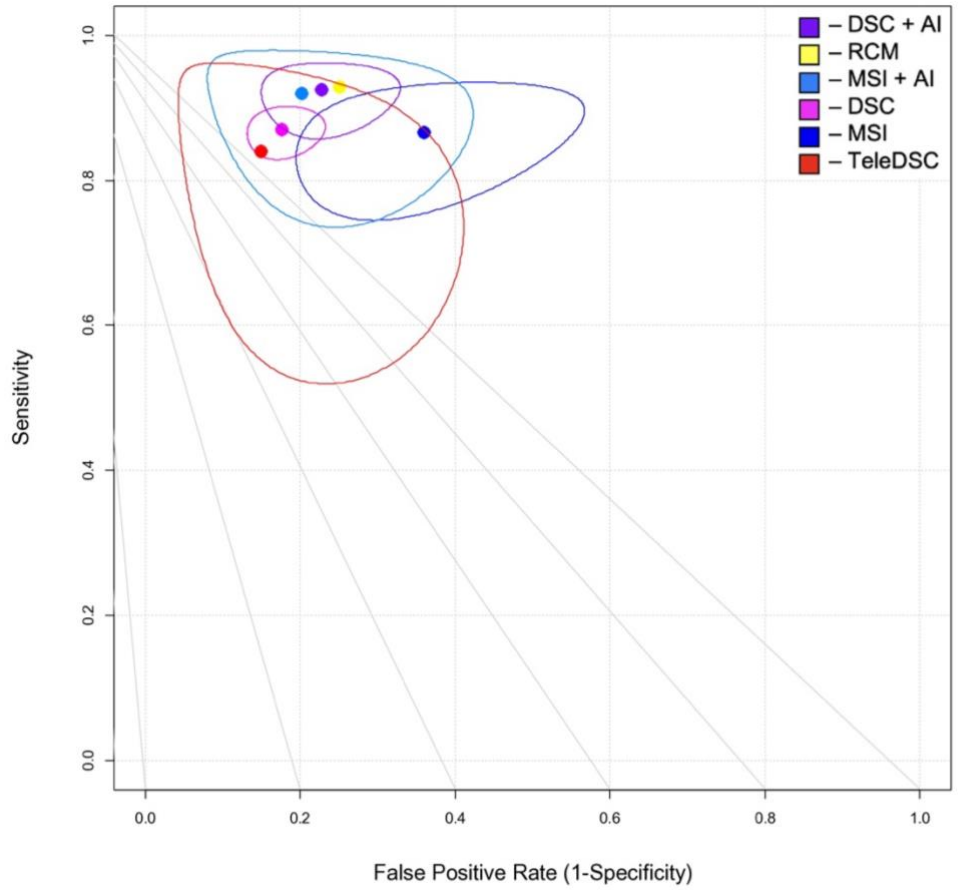

Figure 8. Random-effects diagnostic meta-analysis of optical imaging techniques used in melanoma diagnostics. The sROC curve displays the sensitivity and (1-specificity) of each method, with different colours representing different techniques. Small circles represent summary estimates, and ellipses around circles represent the 95% confidence intervals. The position of the dots and the size of the ellipses provide a visual comparison of the diagnostic accuracy of each method.

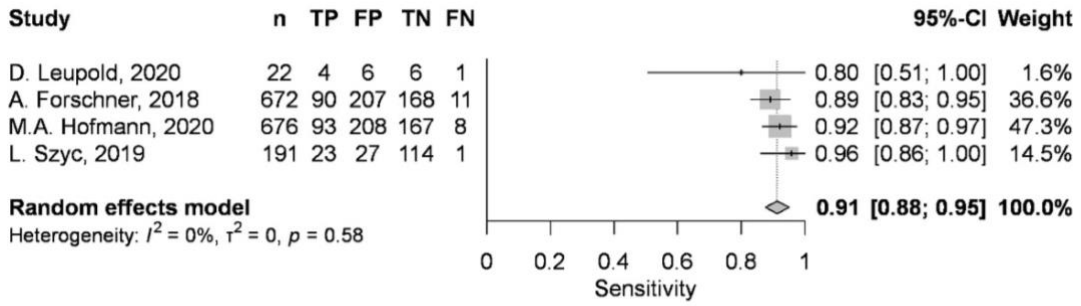

Figure 9. Forest plot representing the sensitivity of studies evaluating the diagnostic performance of DF

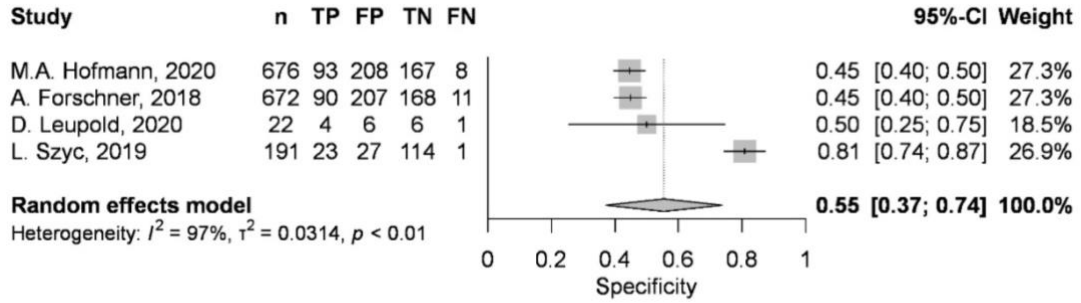

Figure 10. Forest plot representing the specificity of studies evaluating the diagnostic performance of DF

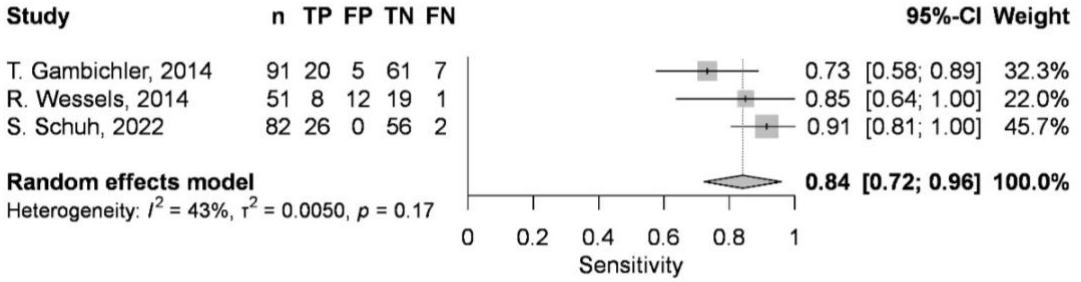

Figure 11. Forest plot representing the sensitivity of studies evaluating the diagnostic performance of OCT

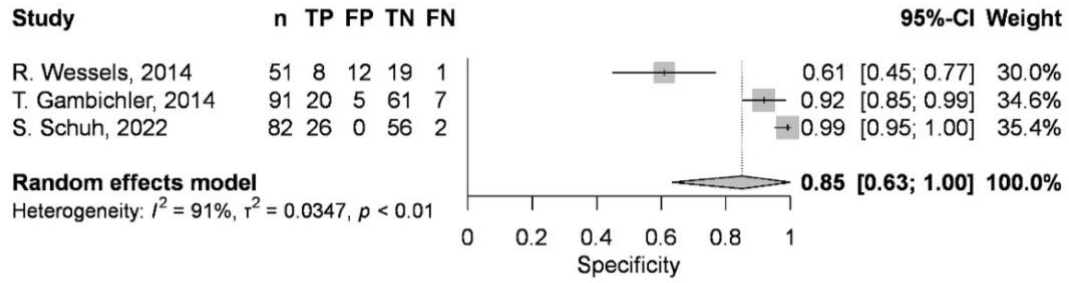

Figure 12. Forest plot representing the specificity of studies evaluating the diagnostic performance of OCT

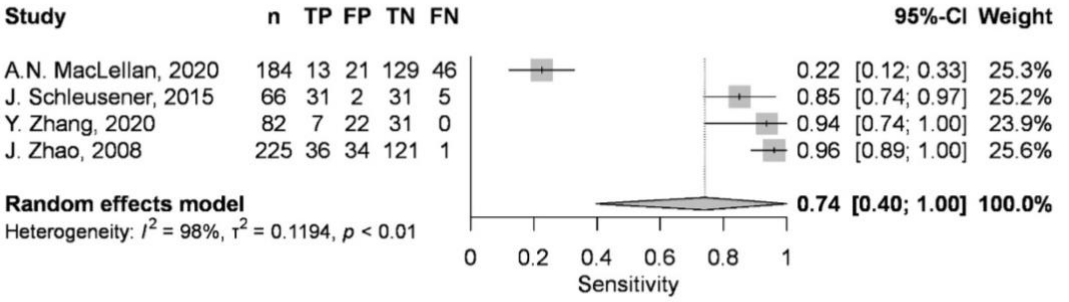

Figure 13. Forest plot representing the sensitivity of studies evaluating the diagnostic performance of RS

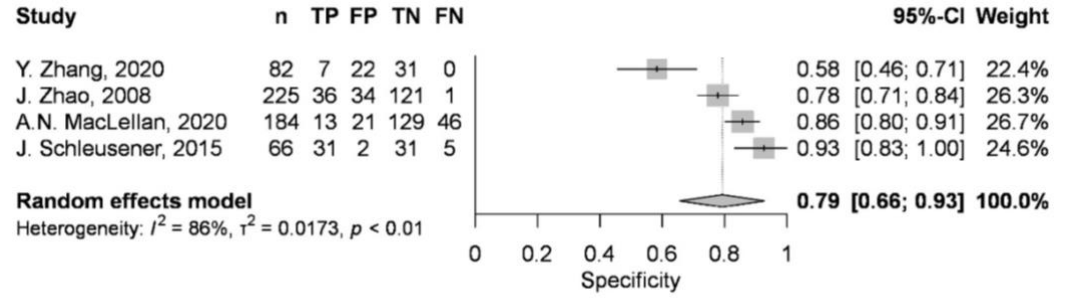

Figure 14. Forest plot representing the specificity of studies evaluating the diagnostic performance of RS

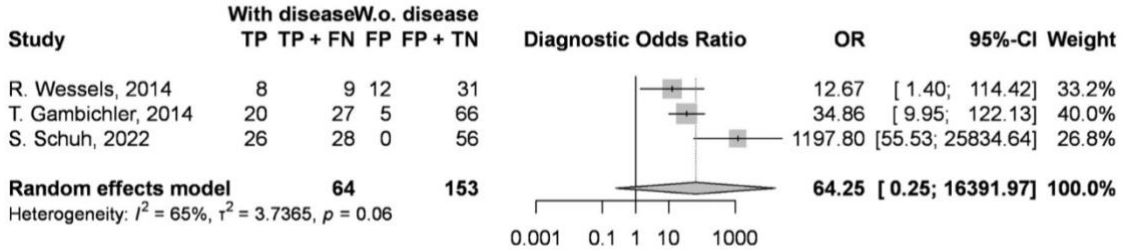

Figure 15. Forest plot for the DOR of studies evaluating the diagnostic accuracy of OCT

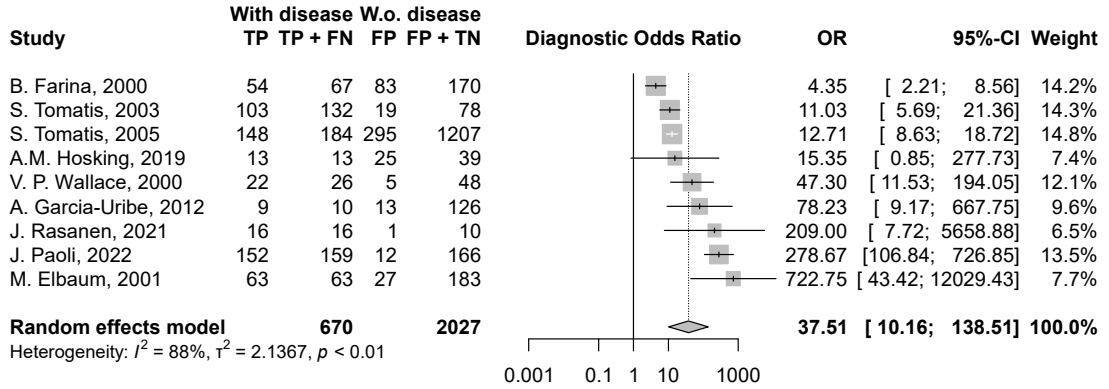

Figure 16. Forest plot for the DOR of studies evaluating the diagnostic accuracy of MSI+AI

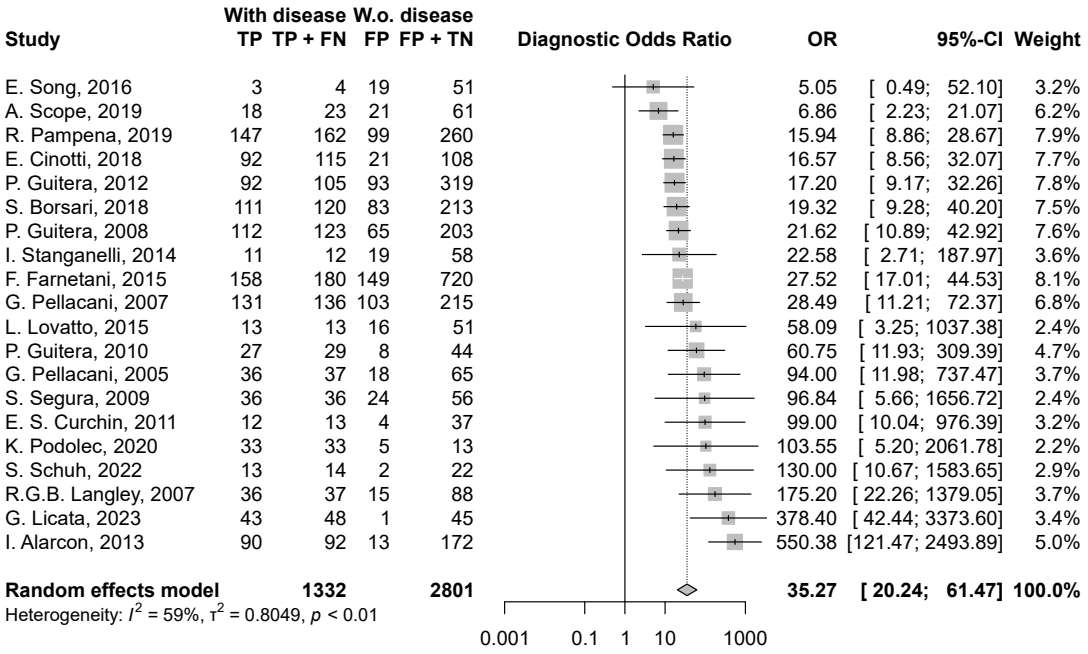

Figure 17. Forest plot for the DOR of studies evaluating the diagnostic accuracy of RCM

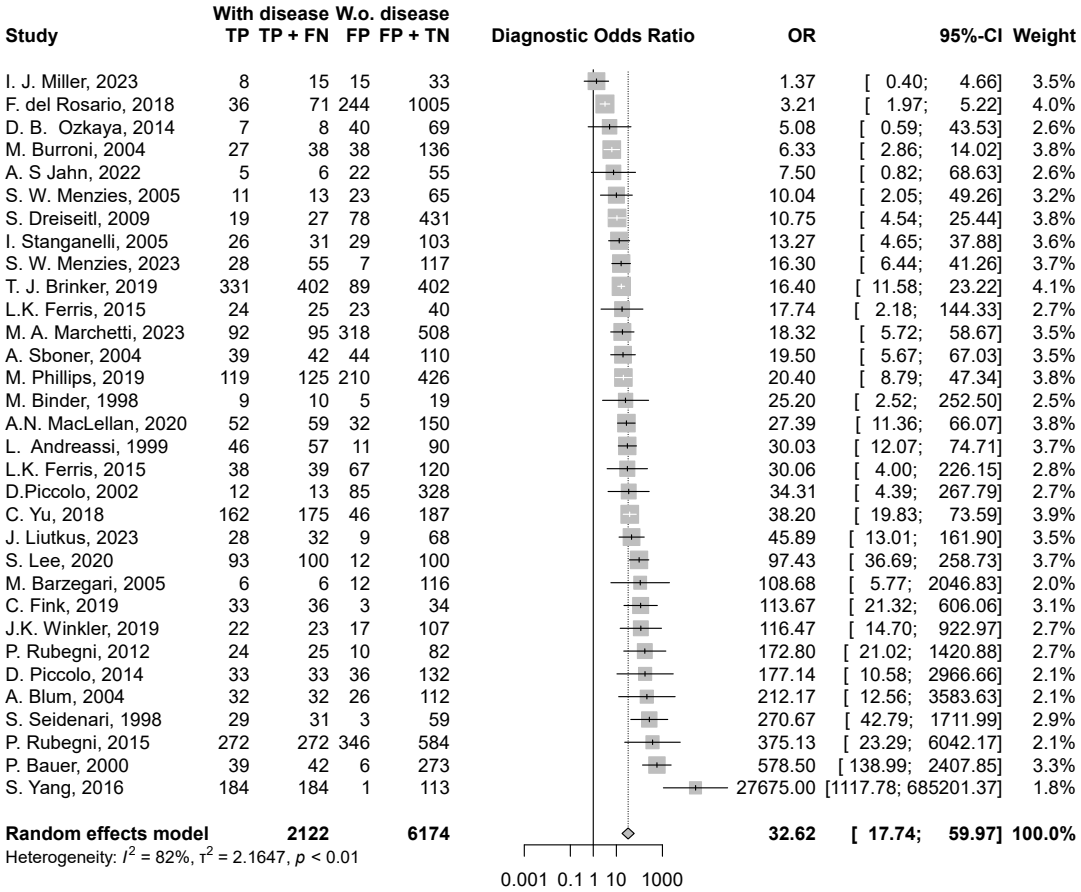

Figure 18. Forest plot for the DOR of studies evaluating the diagnostic accuracy of DSC+AI

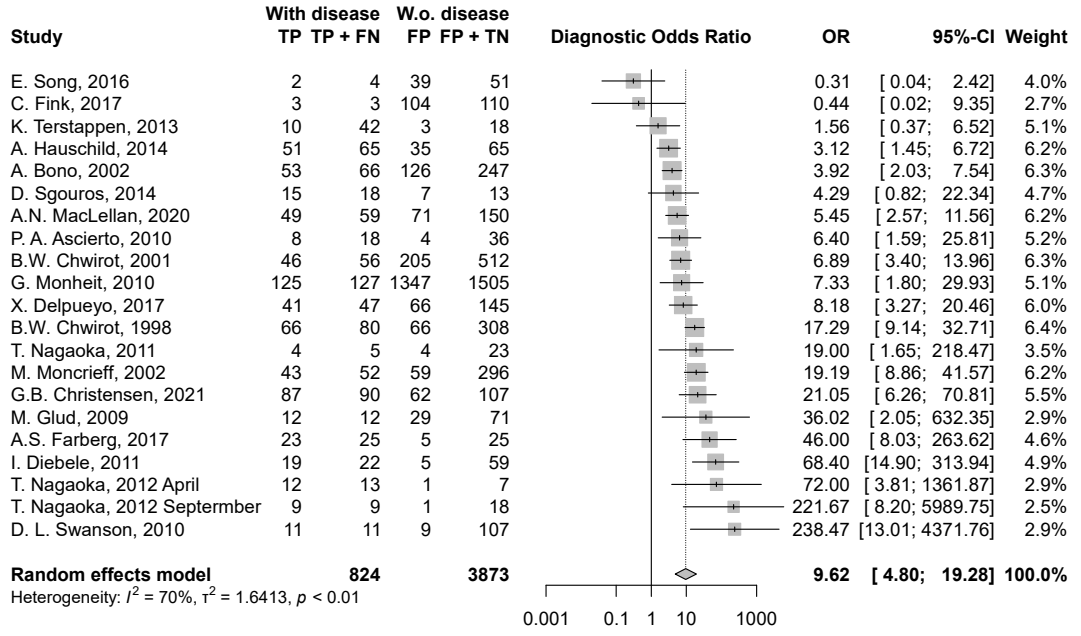

Figure 19. Forest plot for the DOR of studies evaluating the diagnostic accuracy of MSI

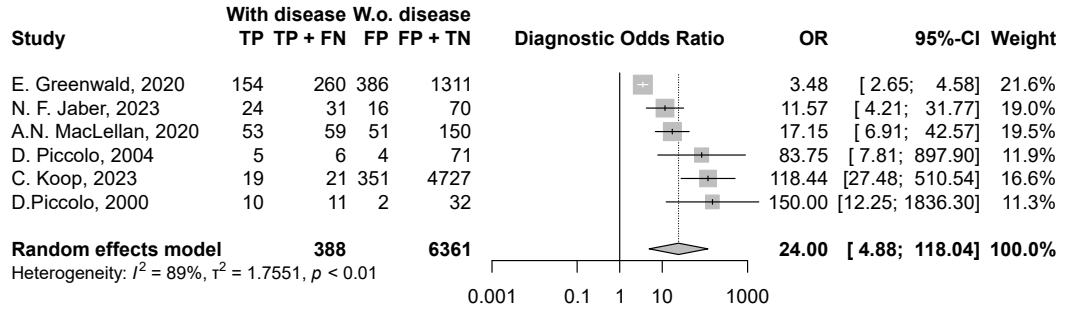

Figure 20. Forest plot for the DOR of studies evaluating the diagnostic accuracy of TeleDSC

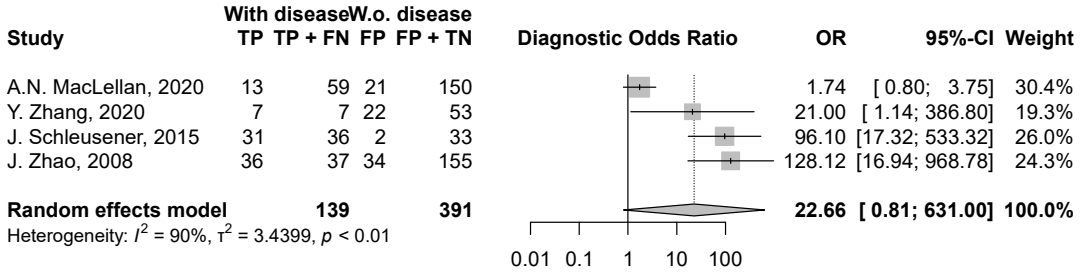

Figure 21. Forest plot for the DOR of studies evaluating the diagnostic accuracy of RS

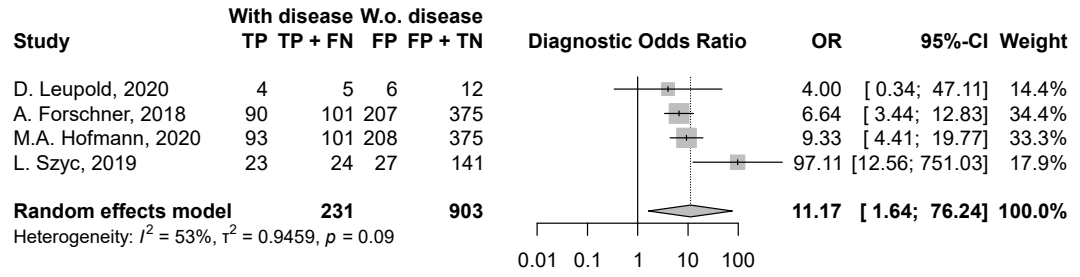

Figure 22. Forest plot for the DOR of studies evaluating the diagnostic accuracy of DF

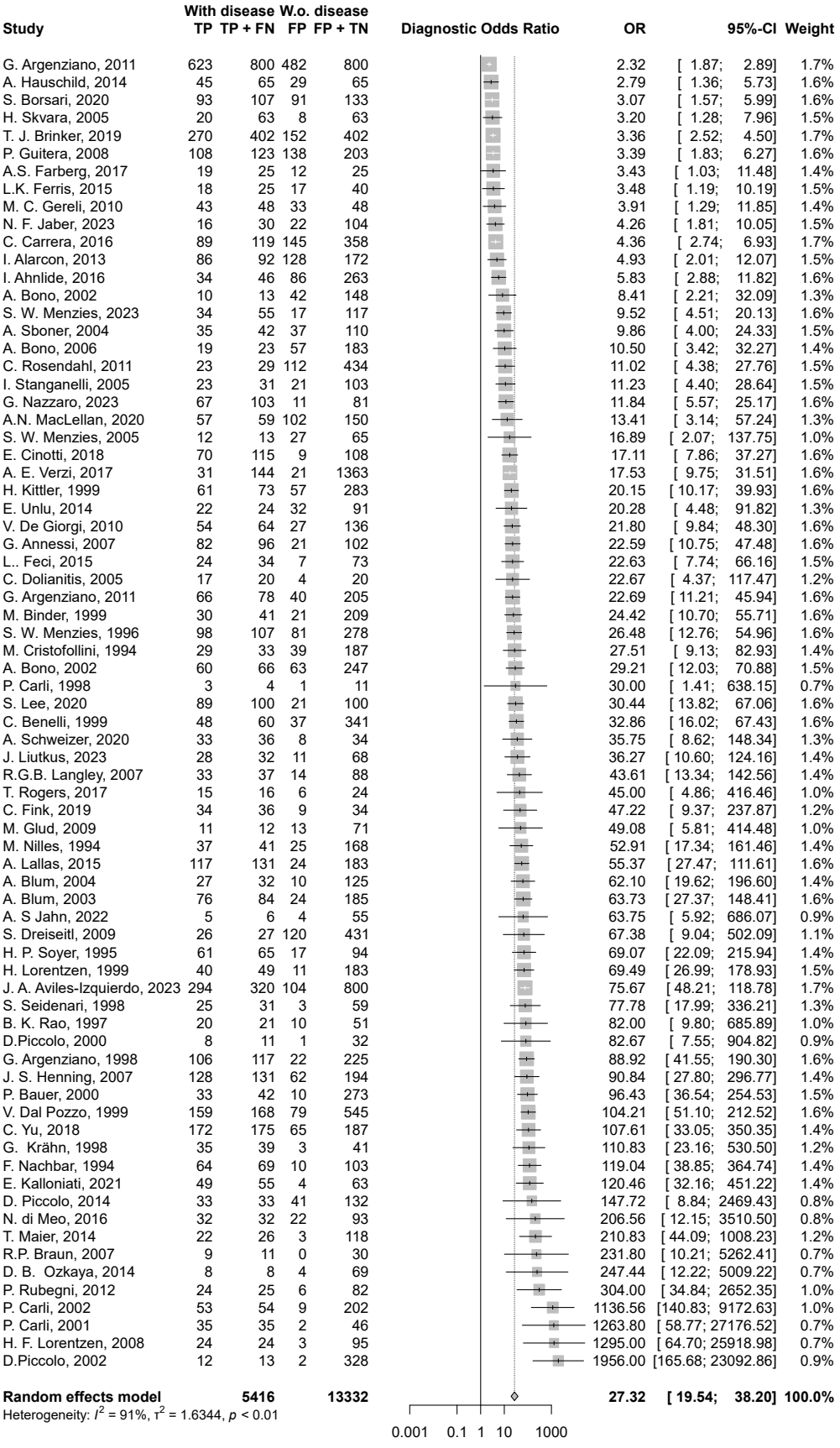

Figure 23. Forest plot for the DOR of studies evaluating the diagnostic accuracy of DSC

Table 5. Ranking of the optical imaging modalities based on the diagnostic odds ratio

Method	Sensitivity	Specificity	PPV*	NPV*	DOR	Level of Evidence for Sensitivity	Level of Evidence for Specificity
OCT	0.84 [0.72; 0.96]	0.85 [0.63; 1.00]	0.71	0.93	**64.25 [0.25; 16391.97]**	⊕⊕◯◯ Low	⊕◯◯◯ Very low
MSI+AI	0.92 [0.82; 0.97]	0.80 [0.67; 0.89]	0.66	0.96	**37.51 [10.16; 138.51]**	⊕◯◯◯ Very low	⊕◯◯◯ Very low
RCM	0.930 [0.9282; 0.9293]	0.749 [0.7475; 0.7504]	0.61	0.96	**35.27 [20.24; 61.47]**	⊕⊕⊕⊕ High	⊕⊕⊕◯ Moderate
DSC+AI	0.93 [0.88; 0.96]	0.77 [0.70; 0.83]	0.64	0.96	**32.62 [17.74; 59.97]**	⊕⊕⊕◯ Moderate	⊕⊕⊕◯ Moderate
DSC	0.87 [0.84; 0.90]	0.82 [0.78; 0.86]	0.68	0.94	**27.32 [19.54; 38.20]**	⊕⊕⊕◯ Moderate	⊕⊕⊕◯ Moderate
TeleDSC	0.84 [0.70; 0.92]	0.85 [0.73; 0.92]	0.71	0.93	**24.00 [4.88; 118.04]**	⊕⊕◯◯ Low	⊕⊕◯◯ Low
RS	0.74 [0.40; 1.00]	0.79 [0.66; 0.93]	0.60	0.88	**22.66 [0.81; 631.00]**	⊕⊕◯◯ Low	⊕⊕◯◯ Low
DF	0.91 [0.88; 0.95]	0.55 [0.37; 0.74]	0.47	0.94	**11.17 [1.64; 76.24]**	⊕◯◯◯ Very low	⊕◯◯◯ Very low
MSI	0.87 [0.78; 0.92]	0.64 [0.49; 0.77]	0.51	0.92	**9.62 [4.80; 19.28]**	⊕⊕◯◯ Low	⊕◯◯◯ Very low

Abbreviations: *DF – Dermatofluoroscopy; DOR – Diagnostic odds ratio; DSC – Dermoscopy; DSC+AI – Dermoscopy+Artificial Intelligence; MSI – Multispectral imaging; MSI+AI – Multispectral imaging+Artificial Intelligence; NPV – Negative predictive value; OCT – Optical coherence tomography; PPV – Positive predictive value; RCM – Reflectance confocal microscopy; RS – Raman spectroscopy TeleDSC – Teledermoscopy. * Average PPV and NPV results at a 30% prevalence rate of melanoma*

Table 6. Summary of the diagnostic accuracy of optical imaging methods solely included in the systematic review

First author, year of publication	Index test (Specific)	Diagnostic accuracy						Level of Evidence		Conclusion of the study
		TP	FN	FP	TN	Sensitivity [95% CI]	Specificity [95% CI]	Sensitivity	Specificity	
I. Bodén, 2013 (192)	NIR-SI spectroscopy (Bruker Matrix F spectrometer)	10	2	2	36	0.83	0.95	⊕⊕◯◯ Low	⊕⊕◯◯ Low	NIR-SI spectroscopy is a promising tool for non-invasive diagnosis of suspect melanoma
L. Lim, 2014 (128)	MSD (RS, DOS, and LIFS)	12	0	0	17	1.00	1.00	⊕◯◯◯ Very low	⊕◯◯◯ Very low	potential for MSD as a clinical diagnostic device
E. Dimitrow, 2009 (93)	MPM (DermaInspect)	19.5	6.5	5.4	21.6	0.75 [0.57; 0.93]	0.80 [0.67; 0.93]	⊕⊕◯◯ Low	⊕⊕◯◯ Low	potential applicability of multiphoton laser tomography in melanoma diagnosis

Abbreviations: *NIR-SI – Near-infrared and skin impedance; MSD – Multimodal spectral diagnosis; RS – Raman spectroscopy; DOS – Diffuse optical spectroscopy; LIFS – Laser-induced fluorescence spectroscopy; MPM – Multiphoton microscopy; TP – True positive; FN – False negative; FP – False positive; TN – True negative; CI – Confidence interval*

8.2.5 Quality assessment

Risk of Bias assessment

The results of the risk of bias assessment and concerns regarding the applicability of each individual study are provided in Table S4 of the Supplementary material to our published article. The proportion of studies evaluated for risk of bias and applicability concerns across the four QUADAS-2 domains is shown in Figure 24. Overall, most studies were judged to be at low risk across all four domains; the highest proportions of high-risk judgments appeared in patient selection (12%) and flow/timing (6%). In both bias and applicability domains, the principal driver of higher-risk or unclear ratings was incomplete reporting of key population characteristics and variability in how the index tests and reference standards were applied.

GRADE assessment

Table 5 presents the level of evidence for sensitivity and specificity of the optical methods included in the meta-analysis, while Table 6 provides this information for the three imaging methods analyzed only in the systematic review. A detailed GRADE assessment for each optical imaging technique is available in the Summary of Findings tables (see the Supplementary material of our article Table S5-15).

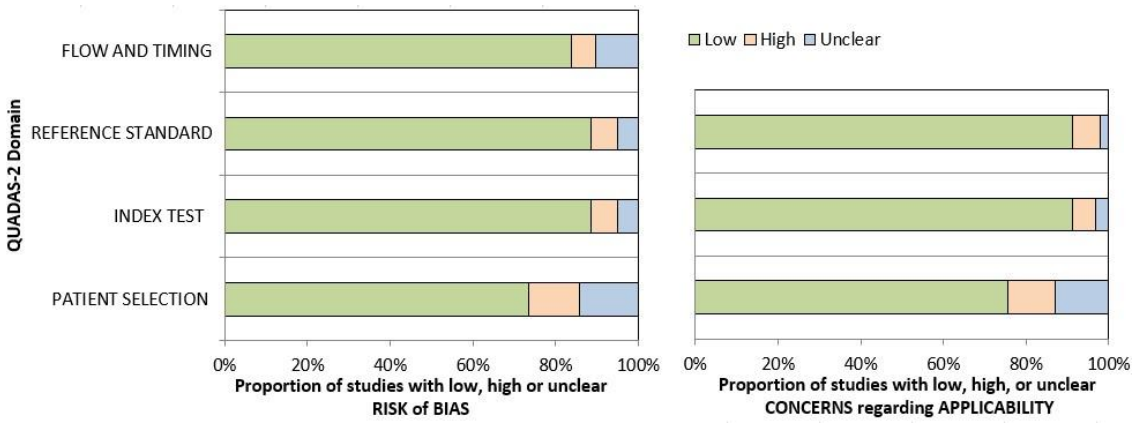

Figure 24. Risk of bias assessment using the QUADAS-2 tool (43)

Publication bias and heterogeneity

Funnel plots indicating the possibility of publication bias can be found in the Supplementary material of the article (see Figures S29-S46). Visual assessment of the funnel plots implied asymmetry and potential publication bias for both sensitivity and specificity of most of the optical methods, except for OCT and MSI+AI.

The detailed heterogeneity data are presented in Figures 9-23, and Figures S1-S12 in the Supplementary material published online. The meta-analyses showed considerable statistical heterogeneity (i.e., I^2>75%), except for the sensitivity of RCM (I^2=59%, substantial statistical heterogeneity), OCT (I^2=43%, moderate statistical heterogeneity), and DF (I^2=0%, no important statistical heterogeneity); also except for the DOR of OCT (I^2=65%, substantial statistical heterogeneity), RCM (I^2=59%, substantial statistical heterogeneity), MSI (I^2=70%, substantial statistical heterogeneity), and DF (I^2=53%, substantial statistical heterogeneity). The P values related to I^2 were mostly $p<0.01$.

9 DISCUSSION

9.1 Summary of findings, international comparisons (including all studies)

The NCCN (195) and EADO (European Association of Dermato-Oncology) (196) provide comprehensive guidelines for the diagnosis and management of melanoma, emphasizing the importance of a thorough dermoscopic examination for initial screening. Our meta-analysis showed that DSC offers balanced diagnostic accuracy, with nearly identical sensitivity and specificity, and an intermediate diagnostic odds ratio, making it a reliable and widely accessible option for early melanoma detection. The moderate level of evidence in the GRADE assessment further supports the technique's reliability. Consequently, DSC continues to be a leading method for melanoma screening. However, achieving proficiency in DSC and enhancing its diagnostic accuracy requires substantial specialization and experience. This highlights the need for more objective and standardized second-step diagnostic tools, which could be provided by emerging optical methods. The findings from the meta-analysis can strengthen our hypothesis that advances in optical imaging and artificial intelligence have the potential to improve melanoma diagnostics. The accuracy of a diagnostic test is primarily influenced by its sensitivity, with RCM and DSC+AI demonstrating the highest sensitivity values in our study. Additionally, RCM and DSC+AI exhibited the highest NPV, making them the most effective at excluding melanoma. RCM also showed strong diagnostic odds ratio and the highest level of evidence for sensitivity, indicating reliable detection of true positive cases. Based on our findings, RCM appears to be the optimal choice for second-step evaluation following DSC screening. It is not only the most sensitive method for diagnosing melanoma that is difficult to assess with DSC, but also the most effective in minimizing the number of benign lesions excised (197). The integration of AI in dermatology is an emerging field that shows great potential for positive outcomes. Our meta-analysis suggests that the integration of AI with DSC significantly improves the diagnostic performance of melanoma detection. This correlates with the findings of Salinas et al. (198) that the diagnostic performance of AI algorithms was better than non-expert dermatologists and comparable to expert dermatologists using only DSC in their clinical practice. In our opinion, DSC+AI is currently best suited for confirming melanoma diagnosis, but in the future, it may surpass standalone DSC in screening as

well. Our analysis revealed similar findings when combining AI with other optical imaging modalities, such as MSI. MSI+AI demonstrated significantly higher sensitivity, specificity, and diagnostic odds ratio values compared to MSI alone. Additionally, MSI+AI achieved the highest NPV, indicating its reliability in excluding melanoma. On the other hand, DF, despite its high sensitivity, exhibited the lowest specificity, with a very low odds ratio and evidence levels, suggesting limited diagnostic reliability. Although OCT displayed the highest DOR of all the modalities evaluated, its sensitivity was only moderate, and the supporting evidence was also low. TeleDSC, while useful for remote diagnostics, showed lower DOR and overall performance compared to most in-person techniques in our meta-analysis. Although PPVs were generally lower than NPVs, OCT and TeleDSC achieved the highest PPV results, suggesting that these methods are more likely to confirm a melanoma diagnosis. RS demonstrated comparatively low performance, with sensitivity, specificity, and DOR results all below those of the other methods, accompanied by very low evidence levels, indicating poorer diagnostic power. While MSD showed 100% sensitivity and specificity, the very low level of evidence suggests that further validation is needed to interpret these results accurately. NIR-SI spectroscopy and MPM demonstrated decent sensitivity and specificity, indicating their potential in specific clinical scenarios, but further research and validation are required to confirm their clinical utility. Although these new optical methods may provide higher-resolution imaging that improves the diagnosis of melanoma, these devices are often expensive and are only available in specialized centers, restricting access to screening. In addition, the interpretation of images requires a high level of expertise, further limiting their use in routine clinical practice (199). Despite their potential, DSC remains the gold standard for screening pigmented lesions due to its accessibility, cost-effectiveness, and proven diagnostic accuracy (200).

Breslow thickness is a key predictor of survival in patients with localized melanoma and helps define the staging and the optimal therapy for patients (201). Our findings revealed that OG-HFUS was superior compared to MSI, demonstrating higher sensitivity, specificity, and overall agreement in predicting Breslow thickness. OG-HFUS demonstrated excellent sensitivity (91.8%) and accurately identified both thin and thick melanomas. This could reduce the risk of underestimating tumor thickness, which could lead to inadequate surgical margins and recurrence. In contrast, MSI showed lower

sensitivity (62.6%), increasing the likelihood of false negatives, which could result in undertreatment. OG-HFUS also excelled in specificity (96.0%), indicating a low rate of false positives and effectively distinguishing melanomas from other pigmented lesions, thus reducing unnecessary excisions. MSI, with lower specificity (81.3%) and moderate agreement ($\kappa = 0.440$), may lead to more false positives and unnecessary procedures, increasing healthcare costs. The observed difference in specificity compared to our previous study with MSI (sensitivity 78%, specificity 89%) (202) may stem from variations in the study cohort, but future algorithm improvements could enhance MSI's performance. When comparing the results of our study with those of Kaikaris et al. (203), notable differences and outcomes are observed. Kaikaris' study, conducted between January 2004 and October 2008, utilized a linear 14 MHz frequency ultrasound sensor to measure melanoma depth in 100 patients diagnosed with stage I-II cutaneous melanoma. Their findings showed varying mean differences, with a larger discrepancy (60 μm) in tumors matching pathological stages I and II. A stronger correlation (r: 0.869) was found in melanomas >2 mm, while thinner melanomas (1-2 mm) showed a weaker correlation (r: 0.283). In contrast, Botar et al. (204) (September 2011 - January 2015) used 40 MHz sonography and strain elastography on 42 melanoma lesions, showing a minimal variance in Breslow depth and ultrasound thickness measurement (mean difference-0.05 mm). A strong correlation was found between elastographic features and strain ratios ($p<0.002$). In Reginelli's study (205), they used ultrasounds with HFUS probes (50-70 MHz) to assess thickness in 14 lesions characterized by distinct dermoscopic features suggestive of nodular melanoma. Their results showed consistent agreement between ultrasound and pathologic thickness in all cases, with positive correlations for both satellite and in-transit lesions as well. Oranges et al. (206) examined 27 melanomas before surgical removal using a 70 MHz HFUS probe in 2014. Their study, which involved two skilled and blinded operators making repeated measurements, found low bias and high correlation between ultrasound and Breslow thickness values, confirming the consistency of ultrasound in preoperative melanoma evaluation. Comparing our results with previous studies underscores the reliability of OG-HFUS, while also highlighting the potential for further improvements in MSI's performance. Overall, OG-HFUS shows great promise as a preoperative tool in melanoma diagnosis and management, warranting further investigation in broader clinical settings.

9.2 Strengths (including all studies)

The key strengths for both of our studies are the clinical relevance and innovation. A meta-analysis and a prospective clinical research both provide an extensive and powerful investigation into novel, non-invasive optical imaging techniques, which are not yet widely implemented in melanoma diagnostics. To the best of our knowledge, this is the first systematic review and meta-analysis to provide a comprehensive analysis of all non-invasive optical imaging techniques for the diagnosis of melanoma. The first study presents real-world, prospective clinical data using two unique prototype devices, offering new insights into preoperative Breslow thickness estimation. We employed standardized data acquisition protocols, clinically relevant reference standards (histology), and blinded evaluations to enhance the internal validity and reduce the risk of bias. Throughout our meta-analysis, we strictly followed the pre-registered PROSPERO protocol to ensure transparency, and a rigorous methodology was applied to achieve a high quality of evidence. Both univariate and multivariate analyses were performed to ensure objectivity in the statistical evaluation. Furthermore, the meta-analysis offers a comprehensive and quantitative summary of diagnostic performance metrics (e.g., sensitivity, specificity, PPV, NPV, DOR, etc.) for multiple emerging technologies, strengthening the evidence for their clinical utility. Another strength across both studies is the robust sample size. In our prospective study, we collected data from a substantial number of patients and lesions, and in our meta-analysis, we included a large, pooled dataset from multiple studies, enhancing the generalizability of our findings. In conclusion, the main strengths of our studies highlight the potential of novel optical imaging techniques to improve melanoma diagnostics and support future clinical research, integration and validation of the diagnostic tools.

9.3 Limitations (including all studies)

In the prospective clinical study, one key limitation lies in the single-center design, which may affect the generalizability of our findings. Additionally, although histological Breslow thickness was used as the reference standard, interobserver variability in HFUS and MSI image interpretation and operator dependence of the devices may have influenced measurement precision. While the prototypes are unique and innovative, we might face limitations regarding reproducibility and external validation in broader clinical settings. Also, the study focused on primary melanomas only, and the performance of OG-HFUS and MSI in evaluating metastatic lesions has yet to be explored. In the meta-analysis, significant methodological heterogeneity - variability in study design, testing strategy, diagnostic thresholds, and imaging device settings - restricted the systematic comparison of all diagnostic techniques, which may affect the consistency and reliability of our results. Differences in sample sizes, patients and pigmented lesions, geographical or institutional practices also increased heterogeneity, which may affect the pooled diagnostic accuracy estimates. The presence of high risk of bias in some of the domains, the low levels of evidence for certain optical techniques, and potential publication bias for both sensitivity and specificity results are also important limitations. Collectively, our two studies illustrate that while optical imaging methods can achieve high diagnostic accuracy in controlled research settings, the identified limitations underscore the need for standardized imaging protocols, multicenter prospective validation studies, and further assessment of the clinical integration, feasibility, and cost-effectiveness of these techniques.

10 CONCLUSION

1) Using shape descriptors and spectral intensity features, we developed a novel MSI-based melanoma classification algorithm.
2) We were the first to employ MSI for melanoma thickness assessment and to classify melanomas into clinically relevant subgroups.
3) In our comparative analysis, OG-HFUS significantly outperformed MSI in the preoperative estimation of Breslow thickness. OG-HFUS yielded lower MSE and higher sensitivity, specificity, PPV, NPV, and Cohen's kappa compared to MSI.
4) OG-HFUS maintained particularly strong accuracy in the Breslow <1 mm subgroup and was least precise in the Breslow between 1-2 mm category.
5) The benefits of MSI and OG-HFUS are that they are handheld, user-friendly, and cost-effective tools for non-invasively estimating Breslow depth, and the measurements can be completed within minutes.
6) Accurate preoperative prediction of Breslow thickness defines the required surgical safety margin, determines the need for concurrent SLNB and the selection of further imaging studies to expedite treatment.
7) To the best of our knowledge, our systematic review and meta-analysis was the first to provide a comprehensive analysis of all non-invasive optical imaging techniques for melanoma diagnosis.
8) RCM and DSC+AI achieved the highest sensitivity and the highest level of evidence for sensitivity, indicating their consistency as diagnostic tools. They also demonstrated the highest NPV values, indicating that these modalities became the most effective in excluding melanoma.
9) The reliability and wide availability of DSC still make it the leading optical method for melanoma screening.
10) RCM and DSC+AI may both be utilized as second-step evaluation methods of pigmented lesions initially suspicious under DSC.
11) Incorporating multimodal imaging techniques after initial DSC screening could potentially maximize diagnostic accuracy.
12) This could mean that the introduction of more precise and reliable techniques as second-step evaluation methods can lead to earlier detection of melanoma, accelerate therapy, and improve the survival rates of melanoma patients.

11 IMPLEMENTATION FOR PRACTICE

Implementing scientific findings into practical recommendations is crucial (220, 221). Medical practitioners and dermatologists should focus on training and skill development in DSC to improve diagnostic accuracy in melanoma screening. In larger dermatological centers, clinicians should also consider integrating multimodal imaging techniques into routine clinical practice after screening with DSC. This approach may provide a more comprehensive evaluation of suspicious pigmented lesions, potentially yielding more precise diagnoses. Adopting more advanced and reliable methods as second-step evaluation, melanoma can be detected earlier, treatment can begin sooner, and patient survival rates may improve. Novel optical imaging tools can also aid in therapy planning after melanoma diagnosis. Based on our results, OG-HFUS could be a reliable, rapid and user-friendly tool in clinical practice to distinguish melanoma depth. Accurate preoperative prediction of Breslow thickness could define the optimal excision margin for the primary melanoma, the need for coincident SLNB, and further imaging procedures. Especially in areas where cosmetic or functional preservation is critical (e.g., face, neck), precise thickness measurements can minimize the need for re-excisions without over-resecting healthy tissue, and surgeons can counsel patients more confidently about expected scar size and functional outcomes. After removing the primary melanoma, the histopathological Breslow measurement determines the need for SLNB. Therefore, if we could know the tumor depth in advance, we could decide whether to perform the SLNB at the same time as primary tumor removal. Thereby reducing the patient's surgical burden and ensuring that nodal status is determined at the outset, which would improve staging. By staging the melanoma earlier, we can more promptly determine which imaging procedures are needed for follow-up and what therapeutic options will be available going forward with the patient. In summary, by maintaining a strong emphasis on implementing innovative multimodal imaging techniques into dermatological practice, healthcare providers could improve early detection and outcomes for patients with melanoma.

12 IMPLEMENTATION FOR RESEARCH

Methodology issues

Although both studies employed rigorous methodological frameworks, we encountered some issues. In our first project, while both modalities showed promising diagnostic performance, several methodological variables (such as subgroup size, lesion size, anatomical site, and imaging conditions) acted as potential confounders. During the analysis of the articles included in the meta-analysis, heterogeneity in the study designs (e.g., retrospective analysis, prospective clinical trials) and variations in testing strategies (e.g., selection of the patients, reference standard test) limited the systematic comparison of the diagnostic techniques.

Study design

Considering the previously mentioned issues, it is advisable to prioritize the evaluation of novel imaging modalities through large-scale, multicenter prospective studies using standardized imaging protocols and histology-based reference standards. A well-organized, multicenter study could overcome current limitations by enhancing the generalizability and external validity of findings, thereby providing diagnostic performance metrics that more accurately reflect real-world clinical variability.

New aspects

Based on our meta-analysis, future research should focus on developing robust artificial intelligence models trained on diverse optical image datasets and validating their diagnostic performance. In this context, the imaging datasets collected in our first study may serve as a training pool for machine learning algorithms for further improvements, both for melanoma diagnosis and estimation of Breslow thickness (222). The results advocate for larger, multicenter prospective validation trials and the development of robust, standardized study designs, particularly those evaluating DSC+AI and RCM in real-world clinical workflows. The studies highlight the need for future research to address feasibility, patient acceptability, workflow integration, and cost-effectiveness of multimodal and AI-supported imaging. These aspects are critical for the successful translation of advanced optical technologies into routine clinical practice.

13 IMPLEMENTATION FOR POLICYMAKERS

Recent advancements in melanoma diagnostics offer a crucial chance for health policymakers to enhance early detection and the diagnostic process. While technological innovation is primarily driven by researchers and developers, it is the responsibility of policymakers to facilitate the integration of these tools into routine clinical workflows with appropriate infrastructure. Due to the increasing incidence of melanoma worldwide and the high prognostic value of precise Breslow thickness assessment, novel diagnostic strategies should be prioritized at multiple levels of prevention. For *primary prevention*, public health initiatives should organise educational programs that raise awareness of melanoma risk, self-examination, and the importance of early professional evaluation. As a form of *secondary prevention*, policymakers should focus on supporting the widespread implementation and access to validated imaging tools, especially in high-risk populations. Policymakers should invest in training programs and infrastructure that support emerging diagnostic technologies in dermatology and oncology centers. Furthermore, ensuring access to these novel technologies in regional settings as well, not just academic centers, is essential to maximizing public health impact. While familiarizing clinicians with the emerging capabilities, they also should promote further research on multimodal and AI-enhanced systems to continuously improve diagnostic accuracy. Regarding *tertiary prevention*, the healthcare system should guarantee that early diagnosis via advanced imaging results in prompt interventions and optimized care pathways. This includes integrating evidence from diagnostic performance studies into guideline updates and nationally applied melanoma care protocols. In conclusion, by maintaining a strong emphasis on multimodal and personalized imaging, healthcare providers could improve early detection and reduce morbidity and mortality related to melanoma.

14 FUTURE PERSPECTIVES

Building on the findings of this thesis, future work will focus on further developing and validating non-invasive optical imaging technologies to improve early melanoma detection. As I have recently started my dermatology residency in Debrecen, we are planning to acquire an OG-HFUS device at the Department of Dermatology, University of Debrecen. This will enable the continuation of data collection and imaging measurements at a new clinical site. The expansion of the study also opens the possibility for a multicenter melanoma cohort investigation, which could enhance the generalizability of our findings and support the development of standardized protocols for non-invasive melanoma diagnostics.

The integration of artificial intelligence into diagnostic workflows remains a critical area of interest. We plan to focus on training and validating machine learning models using real-world clinical datasets. We also plan to further explore the integration of artificial intelligence with non-invasive imaging modalities, including multispectral imaging and dermoscopy, to improve diagnostic accuracy. Our long-term goal is to identify the most effective multimodal imaging approach for routine dermatologic practice.

We plan to regularly reproduce the meta-analysis, following the current concept, as this area is intensively researched, and a significant number of new publications are anticipated each year. We expect our publications to promote more uniform prospective diagnostic accuracy studies that utilize standardized imaging protocols. These changes could enhance the inclusion and synthesis of publications while reducing limitations due to expected lower heterogeneity.

Ultimately, these future directions seek to advance personalized, precise, and minimally invasive oncodermatology.

15 REFERENCES

1. Arnold M, Singh D, Laversanne M, Vignat J, Vaccarella S, Meheus F, et al. Global Burden of Cutaneous Melanoma in 2020 and Projections to 2040. JAMA Dermatology. 2022;158(5):495-503.
2. Kakish DREK, AlSamhori JF, Ayman A, Al-Sawalha M, Hijazeen T, Clementina R, et al. Amelanotic melanoma: Diagnostic challenges, treatment innovations, and the emerging role of in early detection. Journal of Medicine, Surgery, and Public Health. 2025;6:100189.
3. Lo JA, Fisher DE. The melanoma revolution: from UV carcinogenesis to a new era in therapeutics. Science. 2014;346(6212):945-9.
4. Lee KC, Higgins HW, Qureshi AA. Familial risk of melanoma and links with other cancers. Melanoma Management. 2015;2(1):83-9.
5. Shreberk-Hassidim R, Ostrowski SM, Fisher DE. The Complex Interplay between Nevi and Melanoma: Risk Factors and Precursors. International Journal of Molecular Sciences. 2023;24(4):3541.
6. Linos E, Swetter SM, Cockburn MG, Colditz GA, Clarke CA. Increasing burden of melanoma in the United States. J Invest Dermatol. 2009;129(7):1666-74.
7. Dobbinson S, Wakefield M, Hill D, Girgis A, Aitken JF, Beckmann K, et al. Prevalence and determinants of Australian adolescents' and adults' weekend sun protection and sunburn, summer 2003-2004. Journal of the American Academy of Dermatology. 2008;59(4):602-14.
8. D'Souza C, Kramadhari N, Skalkos E, Dutton T, Bailey J. Sun safety knowledge, practices and attitudes in rural Australian farmers: a cross-sectional study in Western New South Wales. BMC Public Health. 2021;21(1):1-10.
9. Swetter SM, Tsao H, Bichakjian CK, Curiel-Lewandrowski C, Elder DE, Gershenwald JE, et al. Guidelines of care for the management of primary cutaneous melanoma. J Am Acad Dermatol. 2019;80(1):208-50.
10. Sober AJ, Chuang TY, Duvic M, Farmer ER, Grichnik JM, Halpern AC, et al. Guidelines of care for primary cutaneous melanoma. J Am Acad Dermatol. 2001;45(4):579-86.

11. Sladden MJ, Balch C, Barzilai DA, Berg D, Freiman A, Handiside T, et al. Surgical excision margins for primary cutaneous melanoma. Cochrane Database Syst Rev. 2009(4):Cd004835.
12. Coit DG, Thompson JA, Albertini MR, Barker C, Carson WE, Contreras C, et al. Cutaneous Melanoma, Version 2.2019, NCCN Clinical Practice Guidelines in Oncology. J Natl Compr Canc Netw. 2019;17(4):367-402.
13. Cassileth BR, Lusk EJ, Tenaglia AN. Patients' perceptions of the cosmetic impact of melanoma resection. Plast Reconstr Surg. 1983;71(1):73-5.
14. Tamošiūnas M, Plorina EV, Lange M, Derjabo A, Kuzmina I, Bļizņuks D, et al. Autofluorescence imaging for recurrence detection in skin cancer postoperative scars. J Biophotonics. 2020;13(3):e201900162.
15. Susan M. Swetter DJ, Mark R. Albertini, Christopher A. Barker, Sarah Bateni et al.¶. National Comprehensive Cancer Network. NCCN Clinical Practice Guidelines in Oncology: Melanoma. Version 2.2025. Cutaneous Melanoma NCCNorg. 2025.
16. Rasheed N. Melanoma awareness programs and their impact on the life of Australian Queenslanders: A concise analysis. Int J Health Sci (Qassim). 2024;18(1):1-3.
17. Davis LE, Shalin SC, Tackett AJ. Current state of melanoma diagnosis and treatment. Cancer Biology & Therapy. 2019;20(11):1366-79.
18. Lopes J, Rodrigues CMP, Gaspar MM, Reis CP. Melanoma Management: From Epidemiology to Treatment and Latest Advances. Cancers (Basel). 2022;14(19).
19. Vestergaard M, Macaskill P, Holt P, Menzies S. Dermoscopy compared with naked eye examination for the diagnosis of primary melanoma: a meta-analysis of studies performed in a clinical setting. British Journal of Dermatology. 2008;159(3):669-76.
20. Argenziano G, Soyer HP, Chimenti S, Talamini R, Corona R, Sera F, et al. Dermoscopy of pigmented skin lesions: results of a consensus meeting via the Internet. Journal of the American Academy of Dermatology. 2003;48(5):679-93.
21. Kittler H, Guitera P, Riedl E, Avramidis M, Teban L, Fiebiger M, et al. Identification of clinically featureless incipient melanoma using sequential dermoscopy imaging. Archives of dermatology. 2006;142(9):1113-9.
22. Wolner ZJ, Yélamos O, Liopyris K, Rogers T, Marchetti MA, Marghoob AA. Enhancing Skin Cancer Diagnosis with Dermoscopy. Dermatol Clin. 2017;35(4):417-37.

23. Jiang Y, Yang M, Wang S, Li X, Sun Y. Emerging role of deep learning-based artificial intelligence in tumor pathology. Cancer communications. 2020;40(4):154-66.
24. Echle A, Rindtorff NT, Brinker TJ, Luedde T, Pearson AT, Kather JN. Deep learning in cancer pathology: a new generation of clinical biomarkers. British journal of cancer. 2021;124(4):686-96.
25. Balch CM, Gershenwald JE, Soong S-j, Thompson JF, Atkins MB, Byrd DR, et al. Final version of 2009 AJCC melanoma staging and classification. Journal of clinical oncology. 2009;27(36):6199.
26. Wachsman W, Morhenn V, Palmer T, Walls L, Hata T, Zalla J, et al. Noninvasive genomic detection of melanoma. Br J Dermatol. 2011;164(4):797-806.
27. Marchesini R, Bono A, Bartoli C, Lualdi M, Tomatis S, Cascinelli N. Optical imaging and automated melanoma detection: questions and answers. Melanoma Res. 2002;12(3):279-86.
28. Welzel J, Schuh S. Noninvasive diagnosis in dermatology. JDDG: Journal der Deutschen Dermatologischen Gesellschaft. 2017;15(10):999-1016.
29. Uppal SK, Beer J, Hadeler E, Gitlow H, Nouri K. The clinical utility of teledermoscopy in the era of telemedicine. Dermatol Ther. 2021;34(2):e14766.
30. Berson M, Gregoire J, Gens F, Rateau J, Jamet F, Vaillant L, et al. High frequency (20 MHz) ultrasonic devices: advantages and applications. European journal of ultrasound. 1999;10(1):53-63.
31. Belfiore MP, Reginelli A, Russo A, Russo GM, Rocco MP, Moscarella E, et al. Usefulness of high-frequency ultrasonography in the diagnosis of melanoma: mini review. Frontiers in Oncology. 2021;11:673026.
32. Serrone L, Solivetti F, Thorel M, Eibenschutz L, Donati P, Catricala C. High frequency ultrasound in the preoperative staging of primary melanoma: a statistical analysis. Melanoma Research. 2002;12(3):287-90.
33. Csány G, Gergely LH, Kiss N, Szalai K, Lőrincz K, Strobel L, et al. Preliminary Clinical Experience with a Novel Optical-Ultrasound Imaging Device on Various Skin Lesions. Diagnostics (Basel). 2022;12(1).
34. Seidenari S, Arginelli F, Manfredini M. Fluorescence lifetime imaging and multiphoton tomography for the study of skin tumors. Skin Research and Technology. 2013;19(1):e567.

35. Spigulis J. Multispectral, fluorescent and photoplethysmographic imaging for remote skin assessment. Sensors. 2017;17(5):1165.

36. Bozsányi S, Farkas K, Bánvölgyi A, Lőrincz K, Fésűs L, Anker P, et al. Quantitative Multispectral Imaging Differentiates Melanoma from Seborrheic Keratosis. Diagnostics (Basel). 2021;11(8).

37. Bliznuks D, Jakovels D, Saknite I, Spigulis J, editors. Mobile platform for online processing of multimodal skin optical images: Using online Matlab server for processing remission, fluorescence and laser speckle images, obtained by using novel handheld device. 2015 International Conference on BioPhotonics (BioPhotonics); 2015: IEEE.

38. Abràmoff MD, Magalhães PJ, Ram SJ. Image processing with ImageJ. Biophotonics international. 2004;11(7):36-42.

39. Bozsányi S, Varga NN, Farkas K, Bánvölgyi A, Lőrincz K, Lihacova I, et al. Multispectral Imaging Algorithm Predicts Breslow Thickness of Melanoma. Journal of Clinical Medicine. 2022;11(1):189.

40. Chandler J, Cumpston M, Li T, Page MJ, Welch V. Cochrane handbook for systematic reviews of interventions. Hoboken: Wiley. 2019.

41. Page MJ, McKenzie JE, Bossuyt PM, Boutron I, Hoffmann TC, Mulrow CD, et al. The PRISMA 2020 statement: an updated guideline for reporting systematic reviews. Bmj. 2021;372:n71.

42. McHugh ML. Interrater reliability: the kappa statistic. Biochem Med (Zagreb). 2012;22(3):276-82.

43. Qu YJ, Yang ZR, Sun F, Zhan SY. [Risk on bias assessment: (6) A Revised Tool for the Quality Assessment on Diagnostic Accuracy Studies (QUADAS-2)]. Zhonghua Liu Xing Bing Xue Za Zhi. 2018;39(4):524-31.

44. Schünemann HJ, Oxman AD, Brozek J, Glasziou P, Jaeschke R, Vist GE, et al. Grading quality of evidence and strength of recommendations for diagnostic tests and strategies. Bmj. 2008;336(7653):1106-10.

45. Chu H, Cole SR. Bivariate meta-analysis of sensitivity and specificity with sparse data: a generalized linear mixed model approach. J Clin Epidemiol. 2006;59(12):1331-2; author reply 2-3.

46. Reitsma JB, Glas AS, Rutjes AW, Scholten RJ, Bossuyt PM, Zwinderman AH. Bivariate analysis of sensitivity and specificity produces informative summary measures in diagnostic reviews. J Clin Epidemiol. 2005;58(10):982-90.

47. Burke DL, Ensor J, Snell KIE, van der Windt D, Riley RD. Guidance for deriving and presenting percentage study weights in meta-analysis of test accuracy studies. Res Synth Methods. 2018;9(2):163-78.

48. Glas AS, Lijmer JG, Prins MH, Bonsel GJ, Bossuyt PMM. The diagnostic odds ratio: a single indicator of test performance. Journal of Clinical Epidemiology. 2003;56(11):1129-35.

49. Balduzzi S, Rücker G, Schwarzer G. How to perform a meta-analysis with R: a practical tutorial. Evid Based Ment Health. 2019;22(4):153-60.

50. Bates D, Mächler M, Bolker B, Walker S. Fitting Linear Mixed-Effects Models Using lme4. ArXiv e-prints. 2014;arXiv:1406.

51. Freeman SC, Kerby CR, Patel A, Cooper NJ, Quinn T, Sutton AJ. Development of an interactive web-based tool to conduct and interrogate meta-analysis of diagnostic test accuracy studies: MetaDTA. BMC Med Res Methodol. 2019;19(1):81.

52. Harrer M, Cuijpers, P., Furukawa, T., & Ebert, D. Doing Meta-Analysis with R: A Hands-On Guide (1st ed.). Chapman and Hall/CRC. 2021.

53. Ahnlide I, Bjellerup M, Nilsson F, Nielsen K. Validity of ABCD Rule of Dermoscopy in Clinical Practice. Acta Derm Venereol. 2016;96(3):367-72.

54. Alarcon I, Carrera C, Palou J, Alos L, Malvehy J, Puig S. Impact of in vivo reflectance confocal microscopy on the number needed to treat melanoma in doubtful lesions. Br J Dermatol. 2014;170(4):802-8.

55. Andreassi L, Perotti R, Rubegni P, Burroni M, Cevenini G, Biagioli M, et al. Digital dermoscopy analysis for the differentiation of atypical nevi and early melanoma: a new quantitative semiology. Arch Dermatol. 1999;135(12):1459-65.

56. Annessi G, Bono R, Sampogna F, Faraggiana T, Abeni D. Sensitivity, specificity, and diagnostic accuracy of three dermoscopic algorithmic methods in the diagnosis of doubtful melanocytic lesions: the importance of light brown structureless areas in differentiating atypical melanocytic nevi from thin melanomas. J Am Acad Dermatol. 2007;56(5):759-67.

57. Argenziano G, Catricalà C, Ardigo M, Buccini P, De Simone P, Eibenschutz L, et al. Seven-point checklist of dermoscopy revisited. Br J Dermatol. 2011;164(4):785-90.
58. Argenziano G, Fabbrocini G, Carli P, De Giorgi V, Sammarco E, Delfino M. Epiluminescence microscopy for the diagnosis of doubtful melanocytic skin lesions. Comparison of the ABCD rule of dermatoscopy and a new 7-point checklist based on pattern analysis. Arch Dermatol. 1998;134(12):1563-70.
59. Argenziano G, Longo C, Cameron A, Cavicchini S, Gourhant JY, Lallas A, et al. Blue-black rule: a simple dermoscopic clue to recognize pigmented nodular melanoma. Br J Dermatol. 2011;165(6):1251-5.
60. Ascierto PA, Palla M, Ayala F, De Michele I, Caracò C, Daponte A, et al. The role of spectrophotometry in the diagnosis of melanoma. BMC Dermatol. 2010;10:5.
61. Avilés-Izquierdo JA, García-Piqueras P, Ciudad-Blanco C, Lozano-Masdemont B, Lázaro-Ochaita P, Bellón-Cano JM, et al. Do not PASS any melanoma without diagnosis: a new simplified dermoscopic algorithm. Int J Dermatol. 2023;62(4):518-23.
62. Barzegari M, Ghaninezhad H, Mansoori P, Taheri A, Naraghi ZS, Asgari M. Computer-aided dermoscopy for diagnosis of melanoma. BMC Dermatol. 2005;5:8.
63. Bauer P, Cristofolini P, Boi S, Burroni M, Dell'Eva G, Micciolo R, et al. Digital epiluminescence microscopy: usefulness in the differential diagnosis of cutaneous pigmentary lesions. A statistical comparison between visual and computer inspection. Melanoma Res. 2000;10(4):345-9.
64. Benelli C, Roscetti E, Dal Pozzo V, Gasparini G, Cavicchini S. The dermoscopic versus the clinical diagnosis of melanoma. European Journal of Dermatology. 1999;9(6):470-6.
65. Binder M, Kittler H, Seeber A, Steiner A, Pehamberger H, Wolff K. Epiluminescence microscopy-based classification of pigmented skin lesions using computerized image analysis and an artificial neural network. Melanoma Res. 1998;8(3):261-6.
66. Binder M, Kittler H, Steiner A, Dawid M, Pehamberger H, Wolff K. Reevaluation of the ABCD rule for epiluminescence microscopy. J Am Acad Dermatol. 1999;40(2):171-6.

67. Biyik Ozkaya D, Onsun N, Su O, Arda Ulusal H, Pirmit S. Pitfalls of an automated dermoscopic analysis system in the differential diagnosis of melanocytic lesions. Acta Dermatovenerol Croat. 2014;22(4):278-83.

68. Blum A, Hofmann-Wellenhof R, Luedtke H, Ellwanger U, Steins A, Roehm S, et al. Value of the clinical history for different users of dermoscopy compared with results of digital image analysis. Journal of the European Academy of Dermatology and Venereology. 2004;18(6):665-9.

69. Blum A, Rassner G, Garbe C. Modified ABC-point list of dermoscopy: A simplified and highly accurate dermoscopic algorithm for the diagnosis of cutaneous melanocytic lesions. J Am Acad Dermatol. 2003;48(5):672-8.

70. Bono A, Bartoli C, Baldi M, Tomatis S, Bifulco C, Santinami M. Clinical and dermatoscopic diagnosis of small pigmented skin lesions. Eur J Dermatol. 2002;12(6):573-6.

71. Bono A, Bartoli C, Cascinelli N, Lualdi M, Maurichi A, Moglia D, et al. Melanoma detection. A prospective study comparing diagnosis with the naked eye, dermatoscopy and telespectrophotometry. Dermatology. 2002;205(4):362-6.

72. Bono A, Tolomio E, Trincone S, Bartoli C, Tomatis S, Carbone A, et al. Micro-melanoma detection: A clinical study on 206 consecutive cases of pigmented skin lesions with a diameter ≤ 3 mm. British Journal of Dermatology. 2006;155(3):570-3.

73. Borsari S, Pampena R, Benati E, Bombonato C, Kyrgidis A, Moscarella E, et al. In vivo dermoscopic and confocal microscopy multistep algorithm to detect in situ melanomas. Br J Dermatol. 2018;179(1):163-72.

74. Borsari S, Peccerillo F, Pampena R, Lai M, Spadafora M, Moscarella E, et al. The presence of eccentric hyperpigmentation should raise the suspicion of melanoma. J Eur Acad Dermatol Venereol. 2020;34(12):2802-8.

75. Braun RP, Gaide O, Oliviero M, Kopf AW, French LE, Saurat JH, et al. The significance of multiple blue-grey dots (granularity) for the dermoscopic diagnosis of melanoma. Br J Dermatol. 2007;157(5):907-13.

76. Brinker TJ, Hekler A, Enk AH, Berking C, Haferkamp S, Hauschild A, et al. Deep neural networks are superior to dermatologists in melanoma image classification. Eur J Cancer. 2019;119:11-7.

77. Burroni M, Sbano P, Cevenini G, Risulo M, Dell'eva G, Barbini P, et al. Dysplastic naevus vs. in situ melanoma: digital dermoscopy analysis. Br J Dermatol. 2005;152(4):679-84.
78. Carli P, De Giorgi V, Argenziano G, Palli D, Giannotti B. Pre-operative diagnosis of pigmented skin lesions: in vivo dermoscopy performs better than dermoscopy on photographic images. J Eur Acad Dermatol Venereol. 2002;16(4):339-46.
79. Carli P, De Giorgi V, Giannotti B. Dermoscopy as a second step in the diagnosis of doubtful pigmented skin lesions: how great is the risk of missing a melanoma? J Eur Acad Dermatol Venereol. 2001;15(1):24-6.
80. Carli P, De Giorgi V, Naldi L, Dosi G, Argenziano G, Fabbrocini G, et al. Reliability and inter-observer agreement of dermoscopic diagnosis of melanoma and melanocytic naevi. European Journal of Cancer Prevention. 1998;7(5):397-402.
81. Carrera C, Marchetti MA, Dusza SW, Argenziano G, Braun RP, Halpern AC, et al. Validity and Reliability of Dermoscopic Criteria Used to Differentiate Nevi From Melanoma: A Web-Based International Dermoscopy Society Study. JAMA Dermatol. 2016;152(7):798-806.
82. Christensen GB, Nagaoka T, Kiyohara Y, Johansson I, Ingvar C, Nakamura A, et al. Clinical performance of a novel hyperspectral imaging device for cutaneous melanoma and pigmented skin lesions in Caucasian skin. Skin Res Technol. 2021;27(5):803-9.
83. Chwirot BW, Chwirot S, Redziński J, Michniewicz Z. Detection of melanomas by digital imaging of spectrally resolved ultraviolet light-induced autofluorescence of human skin. Eur J Cancer. 1998;34(11):1730-4.
84. Chwirot BW, Chwirot S, Sypniewska N, Michniewicz Z, Redzinski J, Kurzawski G, et al. Fluorescence in situ detection of human cutaneous melanoma: study of diagnostic parameters of the method. J Invest Dermatol. 2001;117(6):1449-51.
85. Cinotti E, Labeille B, Debarbieux S, Carrera C, Lacarrubba F, Witkowski AM, et al. Dermoscopy vs. reflectance confocal microscopy for the diagnosis of lentigo maligna. J Eur Acad Dermatol Venereol. 2018;32(8):1284-91.
86. Cristofolini M, Zumiani G, Bauer P, Cristofolini P, Boi S, Micciolo R. Dermatoscopy: usefulness in the differential diagnosis of cutaneous pigmentary lesions. Melanoma Res. 1994;4(6):391-4.

87. Curchin CES, Wurm EMT, Lambie DLJ, Longo C, Pellacani G, Soyer HP. First experiences using reflectance confocal microscopy on equivocal skin lesions in Queensland. Australasian Journal of Dermatology. 2011;52(2):89-97.
88. Dal Pozzo V, Benelli C, Roscetti E. The seven features for melanoma: a new dermoscopic algorithm for the diagnosis of malignant melanoma. Eur J Dermatol. 1999;9(4):303-8.
89. De Giorgi V, Grazzini M, Rossari S, Gori A, Alfaioli B, Papi F, et al. Adding dermatoscopy to naked eye examination of equivocal melanocytic skin lesions: effect on intention to excise by general dermatologists. Clin Exp Dermatol. 2011;36(3):255-9.
90. Del Rosario F, Farahi JM, Drendel J, Buntinx-Krieg T, Caravaglio J, Domozych R, et al. Performance of a computer-aided digital dermoscopic image analyzer for melanoma detection in 1,076 pigmented skin lesion biopsies. J Am Acad Dermatol. 2018;78(5):927-34.e6.
91. Delpueyo X, Vilaseca M, Royo S, Ares M, Rey-Barroso L, Sanabria F, et al. Multispectral imaging system based on light-emitting diodes for the detection of melanomas and basal cell carcinomas: a pilot study (erratum). J Biomed Opt. 2017;22(7):79801.
92. di Meo N, Stinco G, Bonin S, Gatti A, Trevisini S, Damiani G, et al. CASH algorithm versus 3-point checklist and its modified version in evaluation of melanocytic pigmented skin lesions: The 4-point checklist. J Dermatol. 2016;43(6):682-5.
93. Dimitrow E, Ziemer M, Koehler MJ, Norgauer J, König K, Elsner P, et al. Sensitivity and specificity of multiphoton laser tomography for in vivo and ex vivo diagnosis of malignant melanoma. J Invest Dermatol. 2009;129(7):1752-8.
94. Dolianitis C, Kelly J, Wolfe R, Simpson P. Comparative performance of 4 dermoscopic algorithms by nonexperts for the diagnosis of melanocytic lesions. Arch Dermatol. 2005;141(8):1008-14.
95. Dreiseitl S, Binder M, Hable K, Kittler H. Computer versus human diagnosis of melanoma: evaluation of the feasibility of an automated diagnostic system in a prospective clinical trial. Melanoma Res. 2009;19(3):180-4.
96. Elbaum M, Kopf AW, Rabinovitz HS, Langley RG, Kamino H, Mihm MC, Jr., et al. Automatic differentiation of melanoma from melanocytic nevi with multispectral digital dermoscopy: a feasibility study. J Am Acad Dermatol. 2001;44(2):207-18.

97. Emery JD, Hunter J, Hall PN, Watson AJ, Moncrieff M, Walter FM. Accuracy of SIAscopy for pigmented skin lesions encountered in primary care: development and validation of a new diagnostic algorithm. BMC Dermatol. 2010;10:9.
98. Farberg AS, Winkelmann RR, Tucker N, White R, Rigel DS. The Impact of Quantitative Data Provided by a Multi-spectral Digital Skin Lesion Analysis Device on Dermatologists'Decisions to Biopsy Pigmented Lesions. J Clin Aesthet Dermatol. 2017;10(9):24-6.
99. Farina B, Bartoli C, Bono A, Colombo A, Lualdi M, Tragni G, et al. Multispectral imaging approach in the diagnosis of cutaneous melanoma: potentiality and limits. Phys Med Biol. 2000;45(5):1243-54.
100. Farnetani F, Scope A, Braun RP, Gonzalez S, Guitera P, Malvehy J, et al. Skin Cancer Diagnosis With Reflectance Confocal Microscopy: Reproducibility of Feature Recognition and Accuracy of Diagnosis. JAMA Dermatol. 2015;151(10):1075-80.
101. Fazil Jaber N, Jerkovic Gulin S, Seifert O. Analysis of Teledermoscopy and Face-to-Face Examination of Atypical Pigmented Lesions: a Cross-Sectional, Retrospective Study. Dermatol Pract Concept. 2023;13(3).
102. Feci L, Cevenini G, Nami N, Fagiolini A, Perotti R, Miracco C, et al. Influence of Ambient Stressors and Time Constraints on Diagnostic Accuracy of Borderline Pigmented Skin Lesions. Dermatology. 2015;231(3):269-73.
103. Ferris LK, Harkes JA, Gilbert B, Winger DG, Golubets K, Akilov O, et al. Computer-aided classification of melanocytic lesions using dermoscopic images. J Am Acad Dermatol. 2015;73(5):769-76.
104. Fink C, Blum A, Buhl T, Mitteldorf C, Hofmann-Wellenhof R, Deinlein T, et al. Diagnostic performance of a deep learning convolutional neural network in the differentiation of combined naevi and melanomas. J Eur Acad Dermatol Venereol. 2020;34(6):1355-61.
105. Fink C, Jaeger C, Jaeger K, Haenssle HA. Diagnostic performance of the MelaFind device in a real-life clinical setting. J Dtsch Dermatol Ges. 2017;15(4):414-9.
106. Forschner A, Keim U, Hofmann M, Spänkuch I, Lomberg D, Weide B, et al. Diagnostic accuracy of dermatofluoroscopy in cutaneous melanoma detection: results of a prospective multicentre clinical study in 476 pigmented lesions. Br J Dermatol. 2018;179(2):478-85.

107. Gambichler T, Schmid-Wendtner MH, Plura I, Kampilafkos P, Stücker M, Berking C, et al. A multicentre pilot study investigating high-definition optical coherence tomography in the differentiation of cutaneous melanoma and melanocytic naevi. J Eur Acad Dermatol Venereol. 2015;29(3):537-41.
108. Garcia-Uribe A, Zou J, Duvic M, Cho-Vega JH, Prieto VG, Wang LV. In vivo diagnosis of melanoma and nonmelanoma skin cancer using oblique incidence diffuse reflectance spectrometry. Cancer Res. 2012;72(11):2738-45.
109. Gereli MC, Onsun N, Atilganoglu U, Demirkesen C. Comparison of two dermoscopic techniques in the diagnosis of clinically atypical pigmented skin lesions and melanoma: seven-point and three-point checklists. Int J Dermatol. 2010;49(1):33-8.
110. Glud M, Gniadecki R, Drzewiecki KT. Spectrophotometric intracutaneous analysis versus dermoscopy for the diagnosis of pigmented skin lesions: prospective, double-blind study in a secondary reference centre. Melanoma Res. 2009;19(3):176-9.
111. Greenwald E, Tan A, Stein JA, Liebman TN, Bowling A, Polsky D. Real-world outcomes of melanoma surveillance using the MoleMap NZ telemedicine platform. J Am Acad Dermatol. 2021;85(3):596-603.
112. Guitera P, Pellacani G, Crotty KA, Scolyer RA, Li LXL, Bassoli S, et al. The impact of in vivo reflectance confocal microscopy on the diagnostic accuracy of lentigo maligna and equivocal pigmented and nonpigmented macules of the face. Journal of Investigative Dermatology. 2010;130(8):2080-91.
113. Guitera P, Pellacani G, Longo C, Seidenari S, Avramidis M, Menzies SW. In vivo reflectance confocal microscopy enhances secondary evaluation of melanocytic lesions. J Invest Dermatol. 2009;129(1):131-8.
114. Hauschild A, Chen SC, Weichenthal M, Blum A, King HC, Goldsmith J, et al. To excise or not: impact of MelaFind on German dermatologists' decisions to biopsy atypical lesions. J Dtsch Dermatol Ges. 2014;12(7):606-14.
115. Henning JS, Dusza SW, Wang SQ, Marghoob AA, Rabinovitz HS, Polsky D, et al. The CASH (color, architecture, symmetry, and homogeneity) algorithm for dermoscopy. J Am Acad Dermatol. 2007;56(1):45-52.
116. Hofmann MA, Keim U, Jagoda A, Forschner A, Fink C, Spänkuch I, et al. Dermatofluoroscopy diagnostics in different pigmented skin lesions: Strengths and weaknesses. J Dtsch Dermatol Ges. 2020;18(7):682-90.

117. Hosking AM, Coakley BJ, Chang D, Talebi-Liasi F, Lish S, Lee SW, et al. Hyperspectral imaging in automated digital dermoscopy screening for melanoma. Lasers Surg Med. 2019;51(3):214-22.
118. Jahn AS, Navarini AA, Cerminara SE, Kostner L, Huber SM, Kunz M, et al. Over-Detection of Melanoma-Suspect Lesions by a CE-Certified Smartphone App: Performance in Comparison to Dermatologists, 2D and 3D Convolutional Neural Networks in a Prospective Data Set of 1204 Pigmented Skin Lesions Involving Patients' Perception. Cancers. 2022;14(15).
119. Kalloniati E, Cavouras D, Plachouri KM, Geropoulou E, Sakellaropoulos G, Georgiou S. Clinical, dermoscopic and histological assessment of melanocytic lesions: a comparative study of the accuracy of the diagnostic methods. Hippokratia. 2021;25(4):156-61.
120. Kittler H, Seltenheim M, Dawid M, Pehamberger H, Wolff K, Binder M. Morphologic changes of pigmented skin lesions: a useful extension of the ABCD rule for dermatoscopy. J Am Acad Dermatol. 1999;40(4):558-62.
121. Koop C, Kruus P, Hallik R, Lehemets H, Vettus E, Niin M, et al. A country-wide teledermatoscopy service in Estonia shows results comparable to those in experimental settings in management plan development and diagnostic accuracy: A retrospective database study. JAAD International. 2023;12:81-9.
122. Krähn G, Gottlöber P, Sander C, Peter RU. Dermatoscopy and high frequency sonography: two useful non-invasive methods to increase preoperative diagnostic accuracy in pigmented skin lesions. Pigment Cell Res. 1998;11(3):151-4.
123. Lallas A, Kyrgidis A, Koga H, Moscarella E, Tschandl P, Apalla Z, et al. The BRAAFF checklist: a new dermoscopic algorithm for diagnosing acral melanoma. Br J Dermatol. 2015;173(4):1041-9.
124. Langley RG, Walsh N, Sutherland AE, Propperova I, Delaney L, Morris SF, et al. The diagnostic accuracy of in vivo confocal scanning laser microscopy compared to dermoscopy of benign and malignant melanocytic lesions: a prospective study. Dermatology. 2007;215(4):365-72.
125. Lee S, Chu YS, Yoo SK, Choi S, Choe SJ, Koh SB, et al. Augmented decision-making for acral lentiginous melanoma detection using deep convolutional neural networks. J Eur Acad Dermatol Venereol. 2020;34(8):1842-50.

126. Leupold D, Szyc L, Stankovic G, Hofmann M, Scholz M, Forschner A. Dermatofluoroscopy Is Also for Redheads a Sensitive Method of Early Melanoma Detection. Dermatology. 2020;236(6):508-16.
127. Licata G, Brancaccio G, Ronchi A, Borsari S, Longo C, Piana S, et al. Is reflectance confocal microscopy useful in the differential diagnosis of extra facial lentigo maligna? A retrospective multicentric case–control study. Journal of the European Academy of Dermatology and Venereology. 2023.
128. Lim L, Nichols B, Migden MR, Rajaram N, Reichenberg JS, Markey MK, et al. Clinical study of noninvasive in vivo melanoma and nonmelanoma skin cancers using multimodal spectral diagnosis. J Biomed Opt. 2014;19(11):117003.
129. Liutkus J, Kriukas A, Stragyte D, Mazeika E, Raudonis V, Galetzka W, et al. Accuracy of a Smartphone-Based Artificial Intelligence Application for Classification of Melanomas, Melanocytic Nevi, and Seborrheic Keratoses. Diagnostics (Basel). 2023;13(13).
130. Lorentzen H, Weismann K, Petersen CS, Larsen FG, Secher L, Skoødt V. Clinical and dermatoscopic diagnosis of malignant melanoma. Assessed by expert and non-expert groups. Acta Dermato-Venereologica. 1999;79(4):301-4.
131. Lorentzen HF, Løvendahl Eefsen R, Weismann K. Comparison of Classical dermatoscopy and acrylic globe magnifier dermatoscopy. Acta Dermato-Venereologica. 2008;88(2):139-42.
132. Lovatto L, Carrera C, Salerni G, Alós L, Malvehy J, Puig S. In vivo reflectance confocal microscopy of equivocal melanocytic lesions detected by digital dermoscopy follow-up. J Eur Acad Dermatol Venereol. 2015;29(10):1918-25.
133. MacLellan AN, Price EL, Publicover-Brouwer P, Matheson K, Ly TY, Pasternak S, et al. The use of noninvasive imaging techniques in the diagnosis of melanoma: a prospective diagnostic accuracy study. J Am Acad Dermatol. 2021;85(2):353-9.
134. Maier T, Kulichova D, Schotten K, Astrid R, Ruzicka T, Berking C, et al. Accuracy of a smartphone application using fractal image analysis of pigmented moles compared to clinical diagnosis and histological result. J Eur Acad Dermatol Venereol. 2015;29(4):663-7.

135. Marchetti MA, Cowen EA, Kurtansky NR, Weber J, Dauscher M, DeFazio J, et al. Prospective validation of dermoscopy-based open-source artificial intelligence for melanoma diagnosis (PROVE-AI study). NPJ Digit Med. 2023;6(1):127.
136. Menzies SW, Bischof L, Talbot H, Gutenev A, Avramidis M, Wong L, et al. The performance of SolarScan: an automated dermoscopy image analysis instrument for the diagnosis of primary melanoma. Arch Dermatol. 2005;141(11):1388-96.
137. Menzies SW, Ingvar C, Crotty KA, McCarthy WH. Frequency and morphologic characteristics of invasive melanomas lacking specific surface microscopic features. Arch Dermatol. 1996;132(10):1178-82.
138. Menzies SW, Sinz C, Menzies M, Lo SN, Yolland W, Lingohr J, et al. Comparison of humans versus mobile phone-powered artificial intelligence for the diagnosis and management of pigmented skin cancer in secondary care: a multicentre, prospective, diagnostic, clinical trial. Lancet Digit Health. 2023;5(10):e679-e91.
139. Moncrieff M, Cotton S, Claridge E, Hall P. Spectrophotometric intracutaneous analysis: a new technique for imaging pigmented skin lesions. Br J Dermatol. 2002;146(3):448-57.
140. Nachbar F, Stolz W, Merkle T, Cognetta AB, Vogt T, Landthaler M, et al. The ABCD rule of dermatoscopy. High prospective value in the diagnosis of doubtful melanocytic skin lesions. J Am Acad Dermatol. 1994;30(4):551-9.
141. Nagaoka T, Nakamura A, Kiyohara Y, Sota T. Melanoma screening system using hyperspectral imager attached to imaging fiberscope. Annu Int Conf IEEE Eng Med Biol Soc. 2012;2012:3728-31.
142. Nagaoka T, Nakamura A, Okutani H, Kiyohara Y, Koga H, Saida T, et al. Hyperspectroscopic screening of melanoma on acral volar skin. Skin Res Technol. 2013;19(1):e290-6.
143. Nagaoka T, Nakamura A, Okutani H, Kiyohara Y, Sota T. A possible melanoma discrimination index based on hyperspectral data: a pilot study. Skin Res Technol. 2012;18(3):301-10.
144. Nazzaro G, Maronese CA, Casazza G, Giacalone S, Spigariolo CB, Roccuzzo G, et al. Dermoscopic predictors of melanoma in small diameter melanocytic lesions (mini-melanoma): a retrospective multicentric study of 269 cases. Int J Dermatol. 2023;62(8):1040-9.

145. Nilles M, Boedeker RH, Schill WB. Surface microscopy of naevi and melanomas - Clues to melanoma. British Journal of Dermatology. 1994;130(3):349-55.
146. Pampena R, Borsari S, Lai M, Benati E, Longhitano S, Mirra M, et al. External validation and comparison of four confocal microscopic scores for melanoma diagnosis on a retrospective series of highly suspicious melanocytic lesions. J Eur Acad Dermatol Venereol. 2019;33(8):1541-6.
147. Paoli J, Pölönen I, Salmivuori M, Räsänen J, Zaar O, Polesie S, et al. Hyperspectral Imaging for Non-invasive Diagnostics of Melanocytic Lesions. Acta Derm Venereol. 2022;102:adv00815.
148. Pellacani G, Cesinaro AM, Seidenari S. Reflectance-mode confocal microscopy of pigmented skin lesions-improvement in melanoma diagnostic specificity. Journal of the American Academy of Dermatology. 2005;53(6):979-85.
149. Pellacani G, Guitera P, Longo C, Avramidis M, Seidenari S, Menzies S. The impact of in vivo reflectance confocal microscopy for the diagnostic accuracy of melanoma and equivocal melanocytic lesions. J Invest Dermatol. 2007;127(12):2759-65.
150. Phillips M, Marsden H, Jaffe W, Matin RN, Wali GN, Greenhalgh J, et al. Assessment of Accuracy of an Artificial Intelligence Algorithm to Detect Melanoma in Images of Skin Lesions. JAMA Netw Open. 2019;2(10):e1913436.
151. Piccolo D, Crisman G, Schoinas S, Altamura D, Peris K. Computer-automated ABCD versus dermatologists with different degrees of experience in dermoscopy. Eur J Dermatol. 2014;24(4):477-81.
152. Piccolo D, Ferrari A, Peris K, Daidone R, Ruggeri B, Chimenti S. Dermoscopic diagnosis by a trained clinician vs. a clinician with minimal dermoscopy training vs. computer-aided diagnosis of 341 pigmented skin lesions: A comparative study. British Journal of Dermatology. 2002;147(3):481-6.
153. Piccolo D, Smolle J, Argenziano G, Wolf IH, Braun R, Cerroni L, et al. Teledermoscopy--results of a multicentre study on 43 pigmented skin lesions. J Telemed Telecare. 2000;6(3):132-7.
154. Piccolo D, Soyer HP, Chimenti S, Argenziano G, Bartenjev I, Hofmann-Wellenhof R, et al. Diagnosis and categorization of acral melanocytic lesions using teledermoscopy. J Telemed Telecare. 2004;10(6):346-50.

155. Podolec K, Pirowska M, Dyduch G, Wojas-Pelc A. Diagnostic accuracy of reflectance confocal microscopy for pigmented skin lesions presenting dermoscopic features of cutaneous melanoma. Postepy Dermatol Alergol. 2020;37(4):531-4.
156. Rao BK, Marghoob AA, Stolz W, Kopf AW, Slade J, Wasti Q, et al. Can early malignant melanoma be differentiated from atypical melanocytic nevi by in vivo techniques?: Part I. Clinical and dermoscopic characteristics. Skin Res Technol. 1997;3(1):8-14.
157. Räsänen J, Salmivuori M, Pölönen I, Grönroos M, Neittaanmäki N. Hyperspectral Imaging Reveals Spectral Differences and Can Distinguish Malignant Melanoma from Pigmented Basal Cell Carcinomas: A Pilot Study. Acta Derm Venereol. 2021;101(2):adv00405.
158. Rogers T, Marino M, Dusza SW, Bajaj S, Marchetti MA, Marghoob A. Triage amalgamated dermoscopic algorithm (TADA) for skin cancer screening. Dermatol Pract Concept. 2017;7(2):39-46.
159. Rosendahl C, Tschandl P, Cameron A, Kittler H. Diagnostic accuracy of dermatoscopy for melanocytic and nonmelanocytic pigmented lesions. J Am Acad Dermatol. 2011;64(6):1068-73.
160. Rubegni P, Cevenini G, Nami N, Argenziano G, Saida T, Burroni M, et al. Dermoscopy and digital dermoscopy analysis of palmoplantar 'equivocal' pigmented skin lesions in Caucasians. Dermatology. 2012;225(3):248-55.
161. Rubegni P, Feci L, Nami N, Burroni M, Taddeucci P, Miracco C, et al. Computer-assisted melanoma diagnosis: A new integrated system. Melanoma Research. 2015;25(6):537-42.
162. Sboner A, Bauer P, Zumiani G, Eccher C, Blanzieri E, Forti S, et al. Clinical validation of an automated system for supporting the early diagnosis of melanoma. Skin Research and Technology. 2004;10(3):184-92.
163. Schleusener J, Gluszczynska P, Reble C, Gersonde I, Helfmann J, Fluhr JW, et al. In vivo study for the discrimination of cancerous and normal skin using fibre probe-based Raman spectroscopy. Exp Dermatol. 2015;24(10):767-72.
164. Schuh S, Ruini C, Perwein MKE, Daxenberger F, Gust C, Sattler EC, et al. Line-Field Confocal Optical Coherence Tomography: A New Tool for the Differentiation between Nevi and Melanomas? Cancers (Basel). 2022;14(5).

165. Schweizer A, Fink C, Bertlich I, Toberer F, Mitteldorf C, Stolz W, et al. Differentiation of combined nevi and melanomas: Case-control study with comparative analysis of dermoscopic features. J Dtsch Dermatol Ges. 2020;18(2):111-8.
166. Scope A, Dusza SW, Pellacani G, Gill M, Gonzalez S, Marchetti MA, et al. Accuracy of tele-consultation on management decisions of lesions suspect for melanoma using reflectance confocal microscopy as a stand-alone diagnostic tool. J Eur Acad Dermatol Venereol. 2019;33(2):439-46.
167. Segura S, Puig S, Carrera C, Palou J, Malvehy J. Development of a two-step method for the diagnosis of melanoma by reflectance confocal microscopy. J Am Acad Dermatol. 2009;61(2):216-29.
168. Seidenari S, Pellacani G, Pepe P. Digital videomicroscopy improves diagnostic accuracy for melanoma. J Am Acad Dermatol. 1998;39(2):175-81.
169. Sgouros D, Lallas A, Julian Y, Rigopoulos D, Zalaudek I, Longo C, et al. Assessment of SIAscopy in the triage of suspicious skin tumours. Skin Res Technol. 2014;20(4):440-4.
170. Skvara H, Teban L, Fiebiger M, Binder M, Kittler H. Limitations of dermoscopy in the recognition of melanoma. Arch Dermatol. 2005;141(2):155-60.
171. Song E, Grant-Kels JM, Swede H, D'Antonio JL, Lachance A, Dadras SS, et al. Paired comparison of the sensitivity and specificity of multispectral digital skin lesion analysis and reflectance confocal microscopy in the detection of melanoma in vivo: A cross-sectional study. J Am Acad Dermatol. 2016;75(6):1187-92.e2.
172. Soyer HP, Smolle J, Leitinger G, Rieger E, Keri H. Diagnostic reliability of dermoscopic criteria for detecting malignant melanoma. Dermatology. 1995;190(1):25-30.
173. Stanganelli I, Brucale A, Calori L, Gori R, Lovato A, Magi S, et al. Computer-aided diagnosis of melanocytic lesions. Anticancer Res. 2005;25(6):4577-82.
174. Stanganelli I, Longo C, Mazzoni L, Magi S, Medri M, Lanzanova G, et al. Integration of reflectance confocal microscopy in sequential dermoscopy follow-up improves melanoma detection accuracy. Br J Dermatol. 2015;172(2):365-71.
175. Swanson DL, Laman SD, Biryulina M, Ryzhikov G, Stamnes JJ, Hamre B, et al. Optical transfer diagnosis of pigmented lesions. Dermatol Surg. 2010;36(12):1979-86.

176. Szyc Ł, Hillen U, Scharlach C, Kauer F, Garbe C. Diagnostic Performance of a Support Vector Machine for Dermatofluoroscopic Melanoma Recognition: The Results of the Retrospective Clinical Study on 214 Pigmented Skin Lesions. Diagnostics (Basel). 2019;9(3).
177. Terstappen K, Suurküla M, Hallberg H, Ericson MB, Wennberg AM. Poor correlation between spectrophotometric intracutaneous analysis and histopathology in melanoma and nonmelanoma lesions. J Biomed Opt. 2013;18(6):061223.
178. Tomatis S, Bono A, Bartoli C, Carrara M, Lualdi M, Tragni G, et al. Automated melanoma detection: multispectral imaging and neural network approach for classification. Med Phys. 2003;30(2):212-21.
179. Tomatis S, Carrara M, Bono A, Bartoli C, Lualdi M, Tragni G, et al. Automated melanoma detection with a novel multispectral imaging system: results of a prospective study. Phys Med Biol. 2005;50(8):1675-87.
180. Unlu E, Akay BN, Erdem C. Comparison of dermatoscopic diagnostic algorithms based on calculation: The ABCD rule of dermatoscopy, the seven-point checklist, the three-point checklist and the CASH algorithm in dermatoscopic evaluation of melanocytic lesions. J Dermatol. 2014;41(7):598-603.
181. Verzi AE, Quan VL, Walton KE, Martini MC, Marghoob AA, Garfield EM, et al. The diagnostic value and histologic correlate of distinct patterns of shiny white streaks for the diagnosis of melanoma: A retrospective, case-control study. J Am Acad Dermatol. 2018;78(5):913-9.
182. Wallace VP, Bamber JC, Crawford DC, Ott RJ, Mortimer PS. Classification of reflectance spectra from pigmented skin lesions, a comparison of multivariate discriminant analysis and artificial neural networks. Phys Med Biol. 2000;45(10):2859-71.
183. Wessels R, De Bruin DM, Relyveld GN, Faber DJ, Vincent AD, Sanders J, et al. Functional optical coherence tomography of pigmented lesions. Journal of the European Academy of Dermatology and Venereology. 2015;29(4):738-44.
184. Winkler JK, Fink C, Toberer F, Enk A, Deinlein T, Hofmann-Wellenhof R, et al. Association Between Surgical Skin Markings in Dermoscopic Images and Diagnostic Performance of a Deep Learning Convolutional Neural Network for Melanoma Recognition. JAMA Dermatol. 2019;155(10):1135-41.

185. Yang S, Oh B, Hahm S, Chung KY, Lee BU. Ridge and furrow pattern classification for acral lentiginous melanoma using dermoscopic images. Biomedical Signal Processing and Control. 2017;32:90-6.
186. Yu C, Yang S, Kim W, Jung J, Chung KY, Lee SW, et al. Acral melanoma detection using a convolutional neural network for dermoscopy images. PLoS One. 2018;13(3):e0193321.
187. Zhang Y, Moy AJ, Feng X, Nguyen HTM, Sebastian KR, Reichenberg JS, et al. Assessment of Raman Spectroscopy for Reducing Unnecessary Biopsies for Melanoma Screening. Molecules. 2020;25(12).
188. Zhao J, Lui H, McLean DI, Zeng H. Real-time Raman spectroscopy for non-invasive skin cancer detection - preliminary results. Annu Int Conf IEEE Eng Med Biol Soc. 2008;2008:3107-9.
189. Guitera P, Menzies SW, Longo C, Cesinaro AM, Scolyer RA, Pellacani G. In vivo confocal microscopy for diagnosis of melanoma and basal cell carcinoma using a two-step method: analysis of 710 consecutive clinically equivocal cases. J Invest Dermatol. 2012;132(10):2386-94.
190. Ilze D, Ilona K, Janis K, Alexander D, Janis S, editors. Melanoma-nevus differentiation by multispectral imaging. ProcSPIE; 2011.
191. Monheit G, Cognetta AB, Ferris L, Rabinovitz H, Gross K, Martini M, et al. The performance of MelaFind: a prospective multicenter study. Arch Dermatol. 2011;147(2):188-94.
192. Bodén I, Nyström J, Lundskog B, Zazo V, Geladi P, Lindholm-Sethson B, et al. Non-invasive identification of melanoma with near-infrared and skin impedance spectroscopy. Skin Res Technol. 2013;19(1):e473-8.
193. Miller IJ, Stapelberg M, Rosic N, Hudson J, Coxon P, Furness J, et al. Implementation of artificial intelligence for the detection of cutaneous melanoma within a primary care setting: prevalence and types of skin cancer in outdoor enthusiasts. PeerJ. 2023;11:e15737.
194. Diebele I, Kuzmina I, Lihachev A, Kapostinsh J, Derjabo A, Valeine L, et al. Clinical evaluation of melanomas and common nevi by spectral imaging. Biomed Opt Express. 2012;3(3):467-72.

195. National Comprehensive Cancer Network. Melanoma: Cutaneous [Available from: https://www.nccn.org/professionals/physician_gls/pdf/cutaneous_melanoma.pdf.
196. Garbe C, Amaral T, Peris K, Hauschild A, Arenberger P, Basset-Seguin N, et al. European consensus-based interdisciplinary guideline for melanoma. Part 1: Diagnostics: Update 2022. European Journal of Cancer. 2022;170:236-55.
197. Pellacani G, Farnetani F, Ciardo S, Chester J, Kaleci S, Mazzoni L, et al. Effect of Reflectance Confocal Microscopy for Suspect Lesions on Diagnostic Accuracy in Melanoma: A Randomized Clinical Trial. JAMA Dermatol. 2022;158(7):754-61.
198. Salinas MP, Sepúlveda J, Hidalgo L, Peirano D, Morel M, Uribe P, et al. A systematic review and meta-analysis of artificial intelligence versus clinicians for skin cancer diagnosis. NPJ Digit Med. 2024;7(1):125.
199. Jartarkar SR, Patil A, Wollina U, Gold MH, Stege H, Grabbe S, et al. New diagnostic and imaging technologies in dermatology. Journal of Cosmetic Dermatology. 2021;20(12):3782-7.
200. Zalaudek I, Conforti C, Guarneri F, Vezzoni R, Deinlein T, Hofmann-Wellenhof R, et al. Clinical and dermoscopic characteristics of congenital and noncongenital nevus-associated melanomas. J Am Acad Dermatol. 2020;83(4):1080-7.
201. Balch CM, Soong SJ, Gershenwald JE, Thompson JF, Reintgen DS, Cascinelli N, et al. Prognostic factors analysis of 17,600 melanoma patients: validation of the American Joint Committee on Cancer melanoma staging system. J Clin Oncol. 2001;19(16):3622-34.
202. Bozsányi S, Varga NN, Farkas K, Bánvölgyi A, Lőrincz K, Lihacova I, et al. Multispectral imaging algorithm predicts breslow thickness of melanoma. Journal of Clinical Medicine. 2021;11(1):189.
203. Kaikaris V, Samsanavičius D, Maslauskas K, Rimdeika R, Valiukevičienė S, Makštienė J, et al. Measurement of melanoma thickness–comparison of two methods: ultrasound versus morphology. Journal of plastic, reconstructive & aesthetic surgery. 2011;64(6):796-802.
204. Botar-Jid CM, Cosgarea R, Bolboacă SD, Şenilă SC, Lenghel LM, Rogojan L, et al. Assessment of cutaneous melanoma by use of very-high-frequency ultrasound and real-time elastography. American Journal of Roentgenology. 2016;206(4):699-704.

205. Reginelli A, Belfiore MP, Russo A, Turriziani F, Moscarella E, Troiani T, et al. A preliminary study for quantitative assessment with HFUS (High-Frequency Ultrasound) of nodular skin melanoma breslow thickness in adults before surgery: Interdisciplinary team experience. Current radiopharmaceuticals. 2020;13(1):48-55.
206. Oranges T, Janowska A, Scatena C, Faita F, Lascio ND, Izzetti R, et al. Ultra-High Frequency Ultrasound in Melanoma Management: A New Combined Ultrasonographic–Histopathological Approach. Journal of Ultrasound in Medicine. 2023;42(1):99-108.
207. Chaput L, Laurent E, Pare A, Sallot A, Mourtada Y, Ossant F, et al. One-step surgical removal of cutaneous melanoma with surgical margins based on preoperative ultrasound measurement of the thickness of the melanoma. European Journal of Dermatology. 2018;28(2):202-8.
208. Meyer N, Lauwers-Cances V, Lourari S, Laurent J, Konstantinou MP, Lagarde JM, et al. High-frequency ultrasonography but not 930-nm optical coherence tomography reliably evaluates melanoma thickness in vivo: a prospective validation study. British Journal of Dermatology. 2014;171(4):799-805.
209. Pellacani G, Seidenari S. Preoperative melanoma thickness determination by 20-MHz sonography and digital videomicroscopy in combination. Arch Dermatol. 2003;139(3):293-8.
210. De Carvalho N, Welzel J, Schuh S, Themstrup L, Ulrich M, Jemec GB, et al. The vascular morphology of melanoma is related to Breslow index: an in vivo study with dynamic optical coherence tomography. Experimental dermatology. 2018;27(11):1280-6.
211. Huzaira M, Rius F, Rajadhyaksha M, Anderson RR, González S. Topographic variations in normal skin, as viewed by in vivo reflectance confocal microscopy. Journal of investigative dermatology. 2001;116(6):846-52.
212. Lacarrubba F, Verzì AE, Caltabiano R, Broggi G, Di Natale A, Micali G. Discoid lupus erythematosus: Reflectance confocal microscopy features correlate with horizontal histopathological sections. Skin Research and Technology. 2019;25(2):242-4.
213. Chen CS, Elias M, Busam K, Rajadhyaksha M, Marghoob A. Multimodal in vivo optical imaging, including confocal microscopy, facilitates presurgical margin mapping

for clinically complex lentigo maligna melanoma. British Journal of Dermatology. 2005;153(5):1031-6.

214. Yélamos O, Cordova M, Blank N, Kose K, Dusza SW, Lee E, et al. Correlation of handheld reflectance confocal microscopy with radial video mosaicing for margin mapping of lentigo maligna and lentigo maligna melanoma. JAMA dermatology. 2017;153(12):1278-84.

215. Verzì AE, Broggi G, Caltabiano R, Micali G, Lacarrubba F. Line-field confocal optical coherence tomography of lentigo maligna with horizontal and vertical histopathologic correlations. Journal of Cutaneous Pathology. 2023;50(2):118-22.

216. Perez-Anker J, Puig S, Alos L, García A, Alejo B, Cinotti E, et al. Morphological evaluation of melanocytic lesions with three-dimensional line-field confocal optical coherence tomography: correlation with histopathology and reflectance confocal microscopy. A pilot study. Clinical and Experimental Dermatology. 2022;47(12):2222-33.

217. Barragán-Estudillo ZF, Brito J, Chavez-Bourgeois M, Alejo B, Alos L, García AP, et al. Dermoscopy and Reflectance Confocal Microscopy to Estimate Breslow Index and Mitotic Rate in Primary Melanoma. Dermatology Practical & Conceptual. 2022;12(4).

218. Fedorov Kukk A, Wu D, Gaffal E, Panzer R, Emmert S, Roth B. Multimodal system for optical biopsy of melanoma with integrated ultrasound, optical coherence tomography and Raman spectroscopy. Journal of Biophotonics. 2022;15(10):e202200129.

219. Suppa M, Palmisano G, Tognetti L, Lenoir C, Cappilli S, Fontaine M, et al. Line-field confocal optical coherence tomography in melanocytic and non-melanocytic skin tumors. Italian journal of dermatology and venereology. 2023;158(3):180-9.

220. Hegyi P, Erőss B, Izbéki F, Párniczky A, Szentesi A. Accelerating the translational medicine cycle: the Academia Europaea pilot. Nat Med. 2021;27(8):1317-9.

221. Hegyi P, Petersen OH, Holgate S, Erőss B, Garami A, Szakács Z, et al. Academia Europaea Position Paper on Translational Medicine: The Cycle Model for Translating Scientific Results into Community Benefits. J Clin Med. 2020;9(5).

222. Marchesini R, Bono A, Tomatis S, Bartoli C, Colombo A, Lualdi M, et al. In Vivo Evaluation of Melanoma Thickness by Multispectral Imaging and An Artificial Neural Network. A Retrospective Study on 250 Cases of Cutaneous Melanoma. Tumori Journal. 2007;93(2):170-7.

16 BIBLIOGRAPHY

16.1 Publications related to the thesis

1. **Varga, N.N.†**; Boostani, M.†; Farkas, K.; Bánvölgyi, A.; Lőrincz, K.; Posta, M.; Lihacova, I.; Lihachev, A.; Medvecz, M.; Holló, P.; Paragh, Gy.; Wikonkál, N. M.; Bozsányi, S.; & Kiss, N.
   Optically Guided High-Frequency Ultrasound Shows Superior Efficacy for Preoperative Estimation of Breslow Thickness in Comparison with Multispectral Imaging: A Single-Center Prospective Validation Study
   CANCERS
   2024; 16(1), 157. https://doi.org/10.3390/cancers16010157
   Q1, IF: 4.4 (2024)

2. **Varga, N.N.**; Gulyás, L.; Meznerics, F.A.; Barkovskij-Jakobsen, K.S.; Szabó, B.; Hegyi, P.; Bánvölgyi, A.; Medvecz, M.; & Kiss, N.
   Diagnostic Accuracy of Novel Optical Imaging Techniques for Melanoma Detection: A Systematic Review and Meta-Analysis
   INTERNATIONAL JOURNAL OF DERMATOLOGY
   (0011-9059 1365-4632): 2025.
   Advance online publication. https://doi.org/10.1111/ijd.17828
   Q1, IF: 3.2 (2025)

16.2 Publications not related to the thesis

1. Bozsányi, S.; **Varga, N.N.**; Farkas, K.; Bánvölgyi, A.; Lőrincz, K.; Lihacova, I.; Lihachev, A.; Plorina, E. V.; Bartha, Á.; Jobbágy, A.; Kuroli, E.; Paragh, Gy.; Holló, P.; Medvecz, M.; Kiss, N.; & Wikonkál, N. M.
   Multispectral Imaging Algorithm Predicts Breslow Thickness of Melanoma
   JOURNAL OF CLINICAL MEDICINE
   2022; 11(1):189. https://doi.org/10.3390/jcm11010189
   Q1, IF: 3.9 (2022)

2. Bozsányi, S.; Boostani, M.; Farkas, K.; Hamilton-Meikle, P. K.; **Varga, N.N.**; Szabó, B.; Vasanits, F.; Kuroli, E.; Meznerics, F. A.; Lőrincz, K.; Holló, P.; Bánvölgyi, A.; Wikonkál, N. M.; Paragh, Gy.; & Kiss, N.
   Optically Guided High-Frequency Ultrasound to Differentiate High-Risk Basal Cell Carcinoma Subtypes: A Single-Center Prospective Study
   JOURNAL OF CLINICAL MEDICINE
   2023; 12(21):6910. https://doi.org/10.3390/jcm12216910
   Q1, IF: 3.0 (2023)

3. Bozsányi, S.*; Czurkó, N.*; Becske, M.; Kasek, R.; Lázár, B. K.; Boostani, M.; Meznerics, F. A.; Farkas, K.; **Varga, N.N.**; Gulyás, L.; Bánvölgyi, A.; Fehér, B.Á.; Fejes, E.; Lőrincz, K.; Kovács, A.; Gergely, H.; Takács, S.; Holló, P.; Kiss, N.; Wikonkál, N. M.; & Lázár, I.
   Assessment of Frontal Hemispherical Lateralization in Plaque Psoriasis and Atopic Dermatitis
   JOURNAL OF CLINICAL MEDICINE
   2023; 12(13):4194. https://doi.org/10.3390/jcm12134194
   Q1, IF: 3.0 (2023)

4. Jobbágy, A.*; **Varga, N.N.***; Hamilton-Mielke, P. K.; Lőrincz, K.; Meznerics, F.; Blága, K.; Poór, A.; Medvecz, M.; Sárdy, M.; Holló, P.; Wikonkál, N.; Kiss, N.; & Bánvölgyi, A.

   Digitalizáció és modern képalkotó technológiák a bőrgyógyászatban

   BŐRGYÓGYÁSZATI ÉS VENEROLÓGIAI SZEMLE

   2023; 99. évf.: 1. pp. 25-30., 6 p. https://doi.org/10.7188/bvsz.2023.99.1.3

   IF: 0 (2023)

5. Szalai, K.; Farkas, K.; Gergely, H.; **Varga, N.N.**; Magyar, M.; Nagy, Z. Zs.; Fésűs, L.; Bozsányi, Sz.; Jobbágy, A.; Medvecz, M.; Bánvölgyi, A.; Lőrincz, K.; Wikonkál, N.; & Kiss, N.

   Magas frekvenciájú ultrahang, optikai koherencia tomográfia és mágnesesrezonancia képalkotás alkalmazási lehetőségei a bőrgyógyászati gyakorlatban

   BŐRGYÓGYÁSZATI ÉS VENEROLÓGIAI SZEMLE

   2022; 98. évf.: 3. pp. 125-132., 8 p. https://doi.org/10.7188/bvsz.2022.98.3.4

   IF: 0 (2022)

17 ACKNOWLEDGEMENTS

First and foremost, I would like to express my sincere gratitude to all those whose support, encouragement, and expertise have made this scientific work possible.

I am deeply thankful to my supervisors, Norbert Kiss, M.D., Ph.D., and Márta Medvecz, M.D., Ph.D., for their continuous guidance and unwavering support throughout my doctoral studies. Their professional insight and dedication to both academic research and clinical excellence have been a constant source of motivation. I am especially grateful for their understanding and flexibility during the residency training period, which enabled me to balance clinical work and academic commitments.

I would also like to extend my heartfelt thanks to Péter Hegyi, M.D., Ph.D., D.Sc., MAE, director of the Centre for Translational Medicine, Ph.D. Program, for providing me with the opportunity to be part of an inspiring and collaborative research community. His guidance and the methodological support from the Institute have been invaluable in shaping the quality and impact of this dissertation.

I would also like to express my gratitude to the head of the Department of Dermatology, Venereology and Dermatooncology, Semmelweis University - Péter Holló, M.D., Ph.D., D.Sc. - and to the head of the Laboratory of Photobiology and Photocarcinogenesis - Norbert M. Wikonkál, M.D., Ph.D., D.Sc., MAE - for their essential contributions and collaborative spirit throughout my research project.

My sincere appreciation goes to my methodological supervisor, Fanni Meznerics, M.D., Ph.D., for her exceptional mentorship, insightful feedback, and encouragement throughout this journey.

I would like to express my sincere thanks to Szabolcs Bozsányi, M.D., Ph.D., whose encouragement and guidance set me on the path of academic research. It was thanks to his support that I started my Ph.D. journey, and his critical thinking and professionalism greatly influenced the development of my scientific approach.

Special thanks go to my co-investigators – Lili Gulyás, M.D., Mehdi Boostani, M.D., Klára Farkas, M.D., Ph.D., Antal Jobbágy, M.D., Ph.D., András Bánvölgyi, M.D., Ph.D., Kende Lőrincz, M.D., Ph.D. – for their help and support during my research.

I am also especially grateful to Máté Posta, Ph.D., and Bence Szabó, Ph.D., whose expertise in biostatistics and innovative perspective helped refine my research questions and improve the statistical depth of this dissertation.

I extend my gratitude to all members of the Biophotonics Laboratory at the University of Latvia: Marta Lange, Ph.D., Emilija Vija Plorina, Ph.D., Ilze Ļihačova, M.D., Ph.D., Dmitrijs Bļizņuks, M.D., Ph.D., Aleksejs Ļihačovs, M.D., Ph.D., and Janis Spigulis, M.D., Ph.D., D.Sc., for our productive collaboration. I would also like to thank Gergely Csány, Miklós Gyöngy, and Gergely Szikszai-Molnár, as well as the entire team at Dermus Ltd.®, for providing us with the equipment and for the opportunity to collaborate with them.

I would also like to thank Katarina Sofia Barkovskij-Jakobsen, Camille Turquier, Maxime Buitendijk, and Phyllida Hamilton-Meikle for their valuable contribution as student researchers.

In relation to Study I, we would also like to express our gratitude to the dermatopathologists, the surgeons, and the oncological working group of the clinic for their valuable contributions.

I would like to sincerely thank the patients who generously agreed to participate in our research. Their contribution was essential to the success of this work.

Finally, I would like to express my deepest gratitude to my family and friends, whose love, patience, and understanding provided me with strength during the most challenging moments. Their unwavering support has been the foundation upon which this work was built.